Astron. Astrophys. 330, 37–56 (1998)

ASTRONOMY
AND
ASTROPHYSICS

# Molecular gas in galaxies of Hickson compact groups

**S. Leon**[1], **F. Combes**[1], **and T.K. Menon**[2]

[1] DEMIRM, Observatoire de Paris, 61 Av. de l'Observatoire, F-75 014 Paris, France
[2] Department of Physics & Astronomy, Univ. of British Columbia, 2219 Main Mall, Vancouver B.C., V6T 1Z4, Canada

Received 24 April 1997 / Accepted 15 September 1997

**Abstract.** We have observed 70 galaxies belonging to 45 Hickson compact groups in the $^{12}$CO(1→0) and $^{12}$CO(2→1) lines, in order to determine their molecular content. We detected 57 galaxies, corresponding to a detection rate of 81%. We compare the gas content relative to blue and $L_{\rm FIR}$ luminosities of galaxies in compact groups with respect to other samples in the literature, including various environments and morphological types. We find that there is some hint of enhanced $M_{\rm H_2}/L_{\rm B}$ and $M_{\rm dust}/L_{\rm B}$ ratios in the galaxies from compact group with respect to our control sample, especially for the most compact groups, suggesting that tidal interactions can drive the gas component inwards, by removing its angular momentum, and concentrating it in the dense central regions, where it is easily detected. The molecular gas content in compact group galaxies is similar to that in pairs and starburst samples. However, the total $L_{\rm FIR}$ luminosity of HCGs is quite similar to that of the control sample, and therefore the star formation efficiency appears lower than in the control galaxies. However this assumes that the FIR spatial distributions are similar in both samples which is not the case at radio frequencies. Higher spatial resolution FIR data are needed to make a valid comparison. Given their short dynamical friction time-scale, it is possible that some of these systems are in the final stage before merging, leading to ultra-luminous starburst phases. We also find for all galaxy samples that the $H_2$ content (derived from CO luminosity and normalised to blue luminosity) is strongly correlated to the $L_{\rm FIR}$ luminosity, while the total gas content ($H_2$+HI) is not.

**Key words:** galaxies: ISM – galaxies: interactions – galaxies: starburst – galaxies: statistics – radio lines: galaxies

## 1. Introduction

Galaxies are gregarious systems, most of them are gathered in groups or clusters, while only 30% are isolated and 10% are binaries in the field. Nevertheless compact groups (CG) are quite rare and according to Hickson's classification (Hickson, 1982) only 0.1 % of galaxies belong to CGs. Criteria of population (initially four galaxies in the group), isolation (dynamically independent systems) and compactness (separation between galaxies comparable to the sizes of the galaxies) are chosen by Hickson to build his catalog. With these criteria around one hundred CGs were found on the Palomar Observatory Sky Survey red prints.

Compact groups are ideal sites to study the influence of strong dynamical evolution due to environment on molecular cloud formation and star formation efficiency. They appear in projection as the densest galaxy systems known, even denser than the cores of rich clusters, and they show multiple signs of interactions. Due to their high density, and relatively small velocity dispersion, these systems are unstable with regard to merging instability. The dynamical friction time-scale is of the order of $2.10^8$ yrs, and N-body simulations predict their rapid evolution towards a single elliptical massive galaxy (e.g. Barnes 1989). The existence of many such compact groups is therefore a puzzle, and the physical reality of HCG has been questioned (e.g. Mamon 1986, 1987); but evidence of galaxy-galaxy interactions in those groups, either morphologic (Hickson 1990; Mendes de Oliveira 1992), or kinematic (Rubin et al. 1991), speaks in favour of their reality. Latest spectroscopic observations showed that 92 of the original 100 groups have at least three galaxies with recession velocities within 1000 km s$^{-1}$of each other (Hickson et al. 1992). The presence of hot intergalactic gas, detected by X-ray emission centered on some HCGs, is a further confirmation of the existence of these compact groups (Pildis et al. 1995, Ponman et al. 1996).

Most of galaxies that belong to groups are in fact in loose groups of 10-30 galaxies and about 50% of all galaxies belong to loose groups. But loose groups are in their great majority unbound and un-virialised (Gourgoulhon et al. 1992) while their true dynamical state is ambiguous (expanding, collapsing, transient). Clusters of galaxies are more near equilibrium, specially in their centers (about 10% of all galaxies belong to clusters). However, the depth of their potential well leads to high relative velocities between galaxies that reduce the efficiency of galaxy-galaxy encounters. The influence of environment is revealed by the high proportion of ellipticals and lenticulars, and by the HI

*Send offprint requests to*: S. Leon

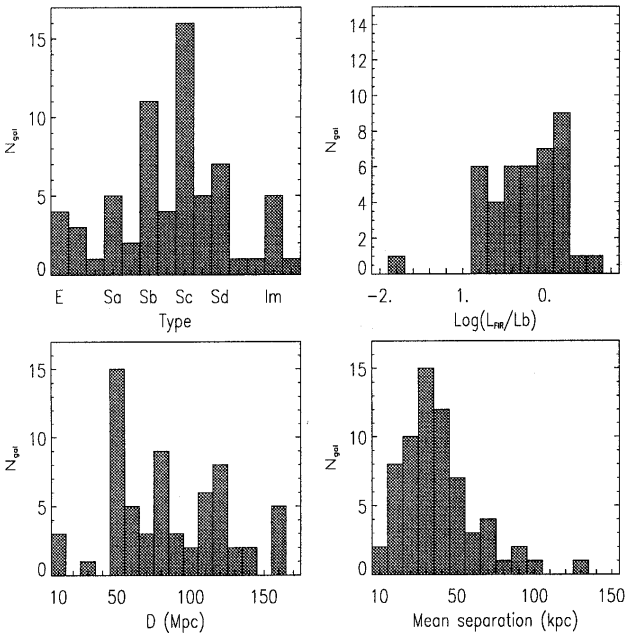


**Fig. 1.** Statistical properties of our CO sample.

gas deficiency of spirals (Dressler 1984, Cayatte et al. 1991). This gas deficiency can be explained by ram-pressure as well as tidal interactions (Combes et al. 1988). No molecular gas deficiency has been detected, either in Virgo (Kenney & Young 1988), or in Coma (Casoli et al. 1991), which suggests that the inner parts of the galaxies are not affected by their environment, since the CO emission essentially comes from the galaxy central regions. However, there could be two compensating effects at play here: the enhancement of CO emission in interacting galaxies (cf Braine et Combes 1993, Combes et al. 1994), and the outer gas stripping, stopping the gas fueling of galaxies.

In compact groups, some HI deficiency has also been reported (Williams & Rood 1987), but no CO emission deficiency, according to a first study by Boselli et al (1996) with the SEST telescope. It is further interesting to investigate whether HCGs are actually sampling the highest densities of galaxies in the Universe. It has been claimed that, even if the CGs are real, we are not sure of their high density, since they could correspond to loose groups with only a high *projected* density through chance alignment of filaments along the line of sight (e.g. Mamon 1992). But no loose groups are observed in HCG neighborhood in the majority (67%) of cases (Rood & Williams 1989). Hickson (1982) found that the groups contain fewer spirals than a comparable sample of field galaxies. The spiral fraction decreases from 60% in the least compact groups to 20% in the most compact. There is also a deficiency of faint galaxies with respect to rich clusters and field. This apparent deficiency is more severe in groups with elliptical first-ranked galaxies. Radio properties of compact groups have been studied by Menon & Hickson (1985) and Menon (1991, 1995). Although the far-infrared and radio luminosities are still highly correlated as for field galaxies, the total radio emission from HCG spirals is relatively lower by a factor 2 in compact group galaxies while the nuclear radio emission is enhanced by a factor of about 10 compared to isolated galaxies. The results suggest a scenario in which interactions among group galaxies produce inflow of gas towards the centers, elevating the star formation there, and consequently the radio and far-infrared emissions. But at the same time the removal of gas and magnetic fields from the extended disks of the galaxies results in a decrease of total radio-emission. Williams & Rood (1987) have observed 51 of the 100 Hickson groups in the HI line, and detected 34 of them. They find that on average a Hickson compact group contains half as much neutral hydrogen as a loose group with a similar distribution of galaxy luminosities and morphological types. This result supports the reality of compact groups as independent dynamical systems and not transient or projected configurations in loose groups. The recent ROSAT survey of HCGs by Ponman et al (1996) also confirms that the groups are intrinsically compact, and not the projection of loose groups. They infer that more than 75% of the HCGs possess hot intragroup gas.

We present here a large CO survey of Hickson group galaxies with the IRAM 30m telescope, and compare the relative gas content and star formation efficiency of CG galaxies with other samples belonging to widely different environments. After describing the observations in Sect. 2, the sample and the data in Sect. 3, we discuss the main conclusions and possible interpretations in Sect. 4.

## 2. Observations

Observations were carried out on 4-10 September 1995 with the 30 meter radiotelescope of the Instituto de Radio Astronomia Milimetrica (IRAM) in Pico Veleta, near Granada in Spain. Single-sideband SIS receivers were tuned for the $^{12}$CO(1→0) and $^{12}$CO(2→1) transitions at respectively 115 and 230 GHz. Weather conditions were excellent during the run with typical effective system temperatures of 300-400 K ($T_{\rm A}^*$ scale ) at 115 GHz and 500-800 K ($T_{\rm A}^*$ scale) at 230 GHz.

For each line a 512 ×1 MHz channel filter bank is used with a velocity resolution of 2.6 km s$^{-1}$smoothed for each spectrum to 10.4 or 20.8 km s$^{-1}$according the quality of each spectrum. At 115 GHz and 230 GHz we assume a HPBW of 22″ and 11″ respectively. Pointing was done frequently on continuum sources with corrections of the offsets up to 8″, providing an accuracy of 3″ (Greve et al, 1996).

The temperature-scale calibration was checked on the sources W3OH, ORIA and IRC+10216 (Mauersberger et al. 1989); except for a transient problem for the 3mm calibration, it remained in a reasonable range providing at least a 20% calibration accuracy. We use the wobbler with a switch cycle of 4 seconds and a beam throw of 90-240″ avoiding off position on another galaxy of the same compact group. Each 12 minutes a chopper wheel calibration was performed on a load at ambient temperature and on a cold load (77 K). The line temperatures are expressed in the $T_{\rm A}^*$ scale, antenna temperature corrected for atmospheric attenuation and rear sidelobes. Baselines were

**Table 1.** General properties of our sample

| Name | type | D (Mpc) | R (kpc) | $D_B$ ($''$) | Log($L_B$) | Log($L_{FIR}$) | $T_d$ (K) | $S_{20cm}$ (mJy) | Log(M(HI)) ($M_\odot$) | Log($M_{dust}$) ($M_\odot$) |
|---|---|---|---|---|---|---|---|---|---|---|
| 2b | cI | 59.3 | 52.5 | 37.6 | 9.95 | 10.16 | 35.8 | | $\leq$10.11 | 6.61 |
| 3c | Sd | 103.0 | 77.0 | 19.8 | 9.93 | 9.93 | 43.3 | | <10.15 | 5.94 |
| 4a | Sc | 112.3 | 57.0 | 67.5 | 10.86 | 10.95 | 34.6 | | | 7.49 |
| 7a | Sb | 57.8 | 45.6 | 80.2 | 10.50 | 10.27 | 35.2 | 12.85 | $\leq$9.28 | 6.76 |
| 7c | SBc | 57.8 | 45.6 | 91.0 | 10.19 | 9.69 | 29.0 | | 9.64 | 6.68 |
| 10a | SBb | 66.6 | 92.9 | 93.6 | 10.76 | 9.01 | | | 9.90 | |
| 10c | Sc | 66.6 | 92.9 | 49.2 | 10.18 | 9.84 | 32.0 | 2.47 | 9.61 | 6.58 |
| 11a† | SBbc | 73.1 | - | 91.9 | 10.70 | 9.64 | 27.7 | | | 6.77 |
| 14b | E5 | 73.5 | 26.9 | 51.9 | 10.23 | <9.12 | | | <9.77 | |
| 14c | Sbc | 73.5 | 26.9 | 15.9 | 9.26 | <9.12 | | | <9.77 | |
| 16a | SBab | 52.5 | 44.6 | 77.1 | 10.50 | 10.53 | 29.6 | 33.18 | 9.48 | 7.47 |
| 16b | Sab | 52.5 | 44.6 | 61.3 | 10.30 | <8.84 | | 2.62 | $\leq$10.07 | |
| 16c | Im | 52.5 | 44.6 | 58.9 | 10.36 | 10.69 | 33.8 | 78.29 | $\leq$10.07 | 7.28 |
| 16d | Im | 52.5 | 44.6 | 63.5 | 10.24 | 10.74 | 33.9 | 30.91 | $\leq$10.07 | 7.33 |
| 19b† | Scd | 56.1 | - | 28.5 | 9.49 | 9.37 | 28.7 | 2.08 | $\leq$9.28 | 6.40 |
| 21a | Sc | 99.8 | 134.9 | 44.9 | 10.51 | 10.36 | 30.8 | | | 7.20 |
| 23b | SBc | 64.0 | 66.1 | 48.7 | 10.00 | 10.09 | 31.2 | 8.01 | $\leq$10.04 | 6.87 |
| 23d | Sd | 64.0 | 66.1 | 26.7 | 9.38 | 9.29 | | 3.18 | <9.26 | |
| 25a | SBc | 84.6 | 47.9 | 51.1 | 10.47 | 9.93 | 32.6 | 4.70 | $\leq$10.09 | 6.62 |
| 25c | Sb | 145.0 | 47.9 | 23.9 | 10.35 | 10.44 | 34.0 | | | 7.03 |
| 27b | SBc | 245.7 | 107.2 | 21.7 | 10.66 | 10.54 | 31.4 | | | 7.32 |
| 31a | Sdm | 57.0 | 49.0 | 33.6 | 9.74 | $\leq$10.32 | | | 9.92 | |
| 31c | Im | 57.0 | 49.0 | 74.5 | 10.68 | $\leq$10.32 | | | 9.85 | |
| 33c | Sd | 103.7 | 24.5 | 18.7 | 9.64 | 9.86 | | 4.58 | $\leq$10.18 | |
| 34b | Sd | 121.8 | 15.5 | 22.2 | 9.71 | $\leq$10.36 | | 6.03 | <10.00 | |
| 37b | Sbc | 88.5 | 28.8 | 40.8 | 10.26 | 9.85 | 28.9 | 1.55 | <8.90 | 6.85 |
| 38b | SBd | 115.1 | 58.9 | 38.4 | 10.38 | $\leq$10.55 | | | $\leq$9.70 | |
| 40a | E3 | 86.7 | 15.1 | 65.3 | 10.66 | $\leq$10.09 | | | <9.70 | |
| 40c | Sbc | 86.7 | 15.1 | 36.5 | 9.98 | 10.07 | 29.4 | 6.03 | <9.70 | 7.03 |
| 40d | SBa | 86.7 | 15.1 | 41.0 | 10.23 | 9.56 | | 6.39 | <9.70 | |
| 40e | Sc | 86.7 | 15.1 | 17.8 | 9.36 | 9.63 | 54.2 | | <9.70 | 5.21 |
| 43a | Sb | 129.8 | 58.9 | 27.0 | 10.34 | 10.18 | 25.4 | 0.95 | <10.16 | 7.56 |
| 43b | SBcd | 129.8 | 58.9 | 25.8 | 10.32 | 10.12 | 26.7 | 1.06 | <10.16 | 7.34 |
| 44a | Sa | 17.3 | 38.0 | 130.5 | 10.03 | 9.31 | 31.4 | 4.77 | 8.64 | 6.09 |
| 44c | SBc | 17.3 | 38.0 | 91.5 | 9.62 | 8.94 | 32.2 | 2.45 | 8.41 | 5.66 |

†not included in our final HCG sample

flat allowing us to subtract only linear polynomials out of the spectra.

## 3. Results

### *3.1. The observed sample*

Our observed sample is composed of 70 galaxies towards 45 compact groups, taken from the catalog of Hickson Compact Groups (HCG, Hickson 1982) . We discarded afterwards 4 galaxies (11a,19b,73a,78a) which appear not to belong to Compact Groups (Hickson, 1992). The galaxies, mostly spirals, are selected for their radio continuum (Menon 1995) and IRAS (Hickson et al. 1989) detections. All the targets are northern sources with $\delta > 0°$. The redshift range from 1200 km s$^{-1}$ up to 18500 km s$^{-1}$ (27b).

If we use $H_0$=75 km s$^{-1}$Mpc$^{-1}$ for the Hubble constant, as adopted in this paper, the mean distance of the sample is 95 Mpc with a standard deviation of 45 Mpc. We present in Fig. 1 the statistical distribution of our sample for distance, type, far infrared ($L_{\rm FIR}$) luminosity and median projected separation.

In Table 1 we display the main properties of the sample. The column headings are the following: name is taken from Hickson classification, type is taken from Hickson et al. (1989), D is the distance computed with a correction for the galactic rotation using a solar galactic velocity of rotation of 250 km s$^{-1}$, R is the median projected galaxy-galaxy separation, $D_B$ indicates the diameter in arcsecs at $\mu_B$ = 24.5 mag.arcsec$^{-2}$, from Hickson et al. (1989), blue luminosity $L_B$ is computed as follows $L_{\rm B}$=12.208-0.4$B^o_T$+log(1+z)+2log(D/Mpc), $L_{\rm FIR}$ luminosity is computed using reprocessed IRAS data from Allam et al. (1996) and following Hickson et al. (1989) derivation, $T_{\rm d}$ is a dust temperature indicator using an emissivity dependence as $\lambda^{-1}$ in the 60-100 $\mu$m IRAS- range, $S_{20cm}$ is the total radio continuum flux density from Menon (1995), neutral hydrogen content has been

**Table 1.** (continued)

| Name | type | D (Mpc) | R (kpc) | $D_B$ ($''$) | Log($L_B$) | Log($L_{FIR}$) | $T_d$ (K) | $S_{20cm}$ (mJy) | Log(M(HI)) ($M_\odot$) | Log($M_{dust}$) ($M_\odot$) |
|---|---|---|---|---|---|---|---|---|---|---|
| 44d | Sd | 17.3 | 38.0 | 70.3 | 9.40 | 8.65 | 39.0 | 2.95 | 8.88 | 4.90 |
| 47a | SBb | 125.3 | 36.3 | 40.3 | 10.52 | 10.27 | 32.1 | 12.25 | <9.78 | 7.00 |
| 49a | Scd | 134.2 | 12.3 | 21.6 | 10.07 | ≤10.12 | | 0.68 | | |
| 49b | Sd | 134.2 | 12.3 | 15.9 | 9.90 | ≤10.12 | | 1.70 | | |
| 55a | E0 | 212.0 | 19.1 | 23.1 | 10.64 | ≤10.58 | | | | |
| 57d | SBc | 120.8 | 72.4 | 44.3 | 10.52 | <10.17 | | 5.09 | | |
| 58a | Sb | 81.5 | 89.1 | 58.2 | 10.56 | 10.59 | 34.3 | 20.71 | 9.75 | 7.14 |
| 59a | Sa | 53.0 | 21.4 | 38.1 | 9.80 | 10.16 | 46.4 | 9.02 | 9.26 | 6.03 |
| 59d | Im | 53.0 | 21.4 | 28.0 | 9.29 | <10.16 | | | ≤8.97 | |
| 61c | Sbc | 51.9 | 28.8 | 57.4 | 10.18 | 10.41 | 33.9 | | ≤9.95 | 6.99 |
| 61d | S0 | 51.9 | 28.8 | 38.7 | 9.95 | <8.92 | | | ≤9.95 | |
| 67b | Sc | 96.8 | 49.0 | 48.1 | 10.58 | 10.28 | 29.7 | 6.70 | 10.20 | 7.22 |
| 67c | Scd | 96.8 | 49.0 | 38.7 | 10.11 | <9.87 | | 13.49 | 9.54 | |
| 68c | SBbc | 33.0 | 33.1 | 134.3 | 10.43 | 9.79 | 28.3 | 2.10 | 9.65 | 6.86 |
| 69a | Sc | 117.9 | 30.2 | 39.4 | 10.33 | <9.48 | | 3.13 | ≤10.15 | |
| 69b | SBb | 117.9 | 30.2 | 23.8 | 10.07 | 10.67 | 41.4 | 6.60 | ≤10.15 | 6.79 |
| 71b | Sb | 120.9 | 50.1 | 22.6 | 10.37 | 10.60 | 35.0 | | <10.27 | 7.11 |
| 73a† | Scd | 76.9 | 100.0 | 76.3 | 10.62 | 9.32 | | | 10.10 | |
| 75b | Sb | 167.3 | 37.2 | 14.8 | 10.65 | <9.89 | | 3.10 | | |
| 75e | Sa | 167.3 | 37.2 | 15.1 | 10.07 | ≤10.22 | | | | |
| 78a† | SBb | 116.8 | - | 51.1 | 10.56 | 10.36 | 31.6 | | 10.29 | 7.12 |
| 79a | E0 | 59.3 | 6.8 | 44.7 | 9.97 | ≤9.82 | | | <9.15 | |
| 79c | S0 | 59.3 | 6.8 | 33.8 | 9.82 | <9.19 | | | <9.15 | |
| 80a | Sd | 126.4 | 25.1 | 25.4 | 10.46 | 10.84 | 33.9 | 20.62 | | 7.43 |
| 82c | Im | 146.7 | 70.8 | 32.9 | 10.58 | 10.59 | 33.9 | 8.33 | <10.09 | 7.17 |
| 88a | Sb | 82.3 | 67.6 | 57.3 | 10.72 | 10.01 | 24.8 | 0.90 | <10.02 | 7.46 |
| 89c | Scd | 120.8 | 58.9 | 24.4 | 10.12 | <9.94 | | | <10.46 | |
| 92c | SBa | 89.0 | 28.2 | 83.2 | 10.73 | 10.15 | 26.0 | 24.74 | 9.90 | 7.46 |
| 93b | SBd | 69.8 | 70.8 | 64.1 | 10.58 | 10.25 | 31.4 | 10.92 | 9.59 | 7.03 |
| 95b | Scd | 160.9 | 30.2 | 25.1 | 10.44 | ≤10.69 | | 3.86 | | |
| 95c | Sm | 160.9 | 30.2 | 26.3 | 10.50 | ≤10.69 | | 6.06 | | |
| 95d | Sc | 160.9 | 30.2 | 16.9 | 10.12 | | | | | |
| 96a | Sc | 119.0 | 30.2 | 61.6 | 10.90 | 11.10 | 39.4 | 200.1 | <10.16 | 7.33 |
| 96c | Sa | 119.0 | 30.2 | 19.8 | 10.04 | <9.88 | | 4.80 | <10.16 | |
| 100a | Sb | 73.3 | 38.0 | 48.9 | 10.43 | 10.273 | 32.6 | 9.17 | 9.74 | 6.95 |

†not included in our final HCG sample

found mainly from Williams & Rood (1987), and some from Huchtmeier & Richter (1989). Concerning $L_{\rm FIR}$ luminosity or HI mass, we indicate in Table 1 the whole group emission preceded by $\leq$, meaning that poor spatial resolution does not allow a separation per galaxy.

### *3.2. Comparison samples*

We compare our results on Hickson compact groups with a 'control' sample, gathering most of the CO data obtained in the literature until now: about 200 galaxies observed by Young et al (1989, 1996) with the FCRAO 14m antenna, by Solomon & Sage (1988) with the FCRAO and NRAO Kitt Peak 12m telescopes, Tinney et al (1990) and by Sage (1993) with the NRAO antenna. This big control sample consists essentially of nearby bright galaxies, and includes a wide range of environment conditions, from isolated and field, to interacting systems. The mergers are also included, and correspond to the highest FIR luminosities of the ensemble. From these observations, we have however separated the Virgo galaxies, and added the results on Coma galaxies (Casoli et al 1991), to build the sample 'Cluster'. We also compare HCG data to more specific samples, such as the isolated pairs from Combes et al (1994), dwarfs from Sage et al (1992), Israel et al (1995) and Leon et al. (1997), and ellipticals from Wiklind et al. (1995), and from Sanders et al. (1991) for the starbursts. For this latter ensemble we separate the pair galaxies to include them in the pair sample. These are noted respectively 'pair', 'dwarf', 'elliptic' and 'starburst' in the various figures of the present work. We have summarized the size of the different samples in Table 2.

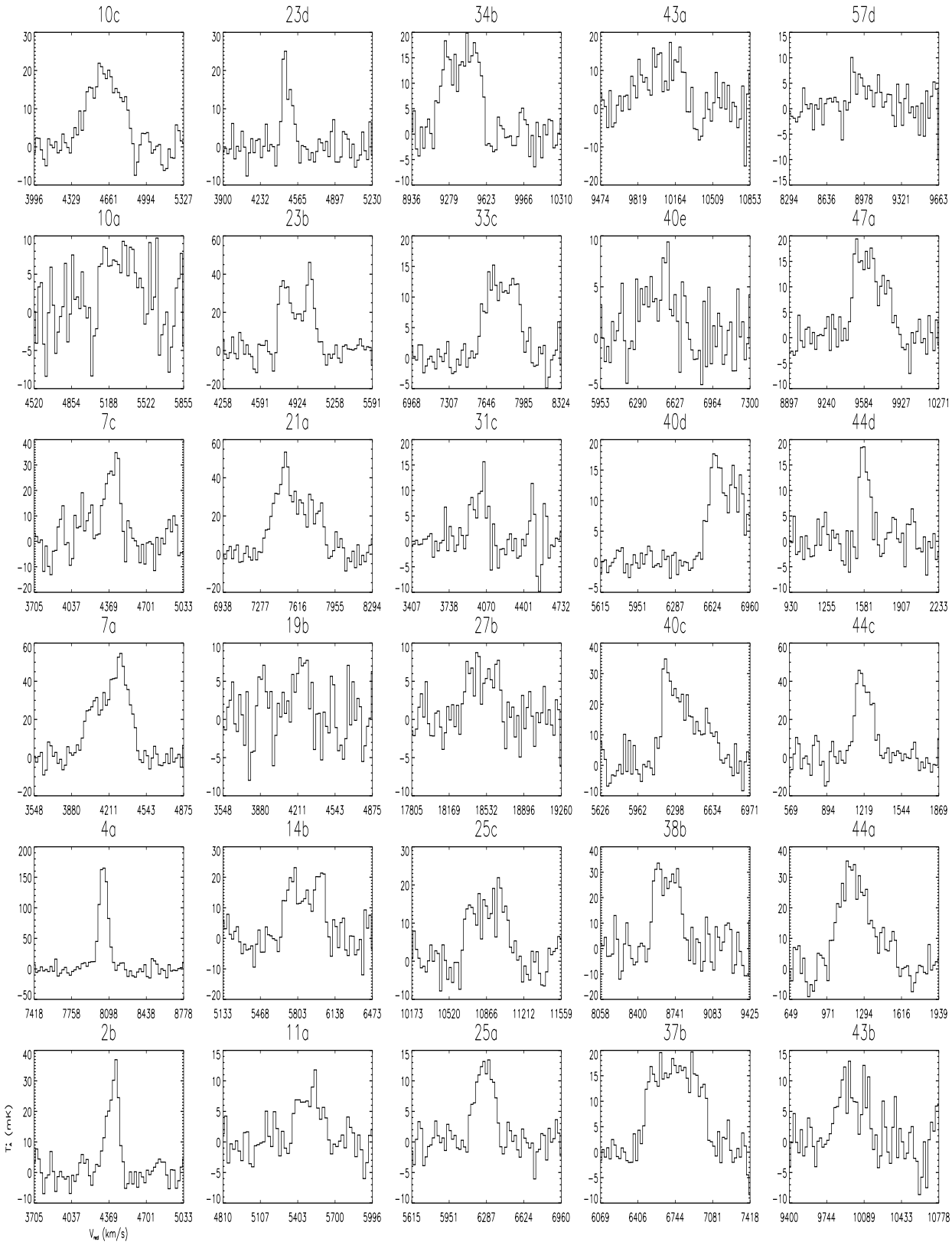


**Fig. 2.** Line profiles of the CO(1-0) emission from our HCG sample. The intensity scale is in units of $T_{\rm A}^{*}$ (mK). The x-axis is the redshift expressed in km s$^{-1}$.

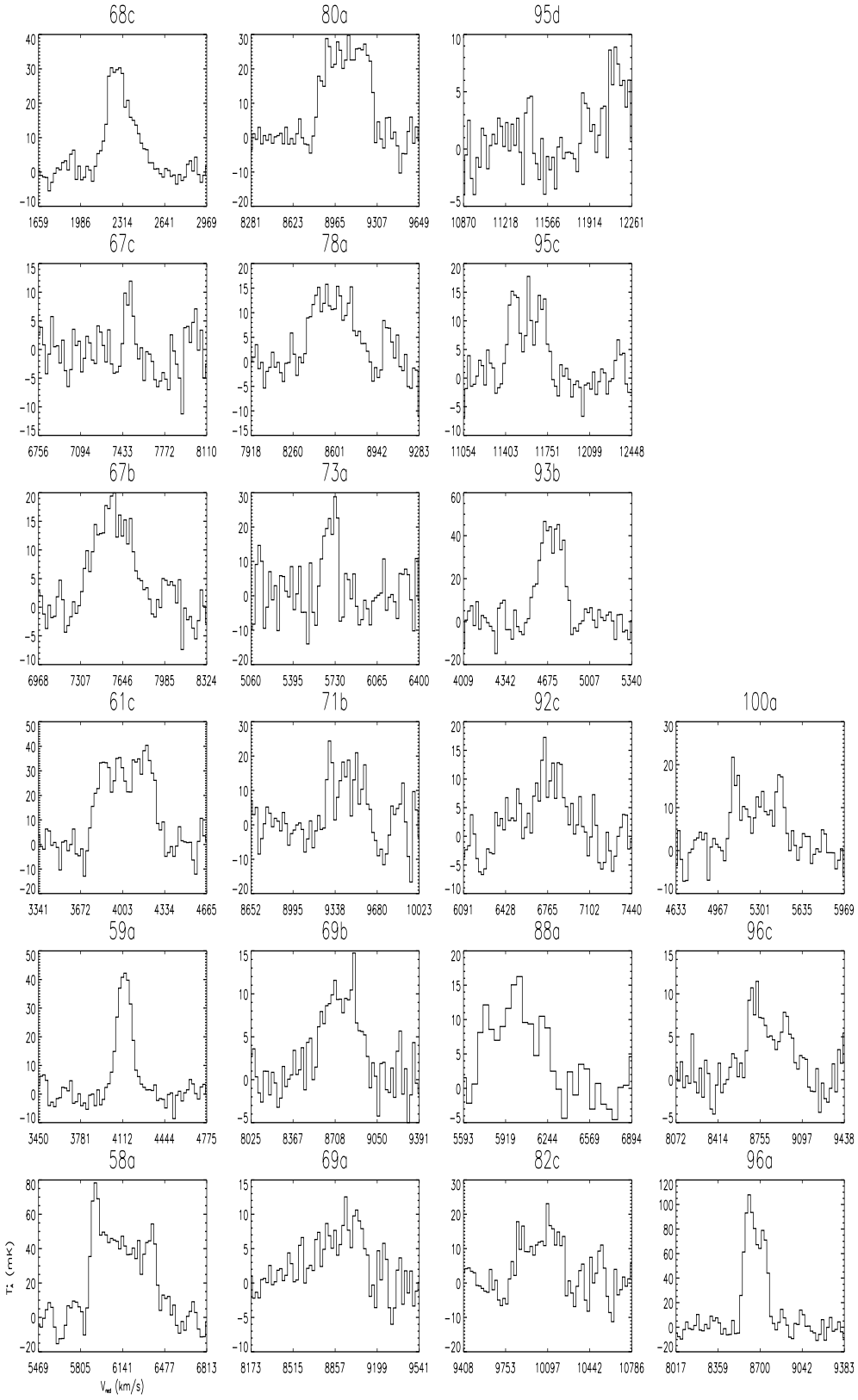


**Fig. 2.** (continued)

**Table 2.** Galaxy numbers in the comparison samples.

| sample | number of galaxies | references |
|---|---|---|
| control | 193 | 7,8,9,10 |
| starburst | 73 | 5 |
| pair | 48 | 2,5 |
| cluster | 40 | 1,10 |
| dwarf | 25 | 3,4,6 |
| elliptic | 18 | 11 |

(1) Casoli et al. (1991), (2) Combes et al. (1994), (3) Israel et al. (1995), (4) Leon et al. (1997), (5) Sanders et al. (1991), (6) Sage et al.(1992), (7) Sage (1993), (8) Solomon & Sage (1988), (9) Tinney et al. (1990), (10) Young et al. (1989,1996), (11) Wiklind et al. (1995)

### *3.3. CO data*

We detected 57 (or 53 in our final HCG sample) galaxies, corresponding to a 80 % detection rate, with 2 detections in $^{12}$CO(2→1) (75e,89c) not detected in $^{12}$CO(1→0), probably due to dilution factor, given the small size of these two galaxies. Some galaxies were detected only in the $^{12}$CO(1→0) line. We reached typically an rms temperature level of 1-8 mK at a smoothed velocity resolution of 10.4-20.8 km s$^{-1}$according to the spectra quality. In Table 3 we present the results of our CO observations: $I_{CO}$ is the velocity-integrated temperature $\int T_a^* dv$ for the $^{12}$CO(1→0) line, or integrated CO intensity, in the $T_A^*$ scale, $\delta I_{CO}$ is the standard error on $I_{CO}$, $T_p$ is the peak antenna temperature, $v_{CO}$ is the intensity-weighted mean heliocentric velocity, FWHM is the full width half maximum of the $^{12}$CO(1→0) spectra, $I_{CO(2-1)}$ is the $^{12}$CO(2→1) integrated intensity and M($H_2$) is the molecular gas mass. The spectra of galaxies detected through the CO(1-0) line are displayed in Fig. 2.

Upper limits of the CO intensities are computed at $3\sigma$ in antenna temperature scale, and with a line width $\delta_{CO}$ guessed from other lines when available from HI lines (Williams & Rood 1987) , and taken as $\delta_{CO}$ = 200 km s$^{-1}$ otherwise. In the case of 40d and 95d we deduced $I_{CO(2-1)}$ and $I_{CO}$ intensities from the fit, because the emission was shifted at the edge of the band. To derive $H_2$ molecular gas content the standard $H_2$/CO conversion factor is adopted (Strong et al. 1988), i.e:

$$N(H_2) = 2.3 \times 10^{20} \int_{line} T_R dv (\mathrm{mol.cm^{-2}}) \quad (1)$$

where $T_R$ is the radiation temperature. Following Gordon et al. (1992) to include size source correction, $H_2$ mass is derived using the expression (see Appendix A):

$$M(H_2) = 5.86 \times 10^4 D^2 K I_{CO} (\mathrm{M_\odot}) \quad (2)$$

where D is the distance in Mpc and K a correction factor for the weighting of the source distribution by the antenna beam. When the source was larger we used a factor 1.38 which leads to a main beam scale. An exponential law was used for modelling radial distribution of molecular gas with a scale length h=$D_B$/10, the molecular gas following approximately the optical light distribution (Young & Scoville, 1982) i.e. the assumed gas surface density $\mu(r)$ is

$$\mu(r) \propto e^{-\frac{r}{h}} \quad (3)$$

We could expect a more radially concentrated molecular distribution in these tidally perturbed galaxies, but if we compare with a gaussian distribution, there is at most a difference of a factor 1.5 on the factor K. Thus M($H_2$) will only be slightly overestimated through this effect. We note that this assumption works well for the group 16 where we have mapped in CO the whole galaxies. For 75e and 80c a mean ratio $I_{CO}/I_{CO(2-1)}$=1.35 is used to derive $I_{CO}$ intensity in the $^{12}$CO(1→0) line. The mean $H_2$ mass versus galaxy morphological type is presented in Fig. 3.

### *3.4. Average gas content and star formation efficiency*

From Table 3, average quantities can be derived to characterize the HCGs as a class. To avoid size effects and artificial correlations induced by uncertain distances, we used quantities normalised to the blue luminosity $L_B$. All the quantities are displayed in logarithm in the Table 4. The average $L_{FIR}/L_B$ ratio is -0.16 ± 0.45 for HCG, which indicates a moderate star forming enhancement over isolated galaxies, as already found by Sulentic & de Mello Rabaça (1993). It should be emphasized here that the comparison among samples using the blue luminosity normalised values of the total $L_{FIR}$ and $M_{H_2}$ by Sulentic & De Mello Rabaça (1993) assumes that the spatial distributions of these two quantities are similar to the blue luminosity distributions. However as stressed by Menon (1995) in his comparison of radio properties of HCG spirals and isolated spirals the differences in spatial distributions have to be taken into account for any meaningful comparison of sample properties. The average $M_{H_2}/L_B$ ratio is found to be -0.61 ± 0.39, which has to be compared with the -1.19 value of Boselli et al. (1996). This difference might be due to the small size of the Boselli et al. sample and also to the fact that they do not take into account the correction of galaxy-to-beam size ratio in deriving the $H_2$ content. Yun et al (1997) also reported an apparent CO emission deficiency in two HCG groups that they mapped with the OVRO interferometer (31c and 92c). However, their observations are missing extended CO emission, and they find 2 and 10 times less $M_{H_2}$ than the present work, for 31c and 92c respectively.

The $L_{FIR}/M_{H_2}$ ratio is widely used as an indicator of the star formation efficiency (SFE) (Young et al. 1986). While our present control has an average SFE of 0.67 ± 0.38, the HCG sample has an SFE of 0.39 ± 0.33, which confirms the only moderate triggering effect of the compact environment on the global star formation.This value has to be compared with the high ratio of 1.24 for the starburst sample which is about 7 times higher. If we take as indicator of SFE the ratio $L_{FIR}/(M_{H_2}+M_{HI})$, as proposed by Sulentic & de Mello Rabaça (1993), no star formation enhancement is observed with a mean ratio of -0.02 ± 0.40; however, this value is then uncertain, due to the available sample

**Table 3.** Molecular data

| Name | $I_{CO}$ (K km s$^{-1}$) | $\delta I_{CO}$ (K km s$^{-1}$) | $T_p$ (mK) | $v_{CO}$ (km s$^{-1}$) | FWHM (km s$^{-1}$) | $I_{CO(2-1)}$ (K km s$^{-1}$) | Log(M($H_2$)) ($M_\odot$) | Log($L_{FIR}/M_{H_2}$) ($L_\odot/M_\odot$) | Log($L_{FIR}/(M_{gas})$) ($L_\odot/M_\odot$) |
|---|---|---|---|---|---|---|---|---|---|
| 2b | 3.90 | 0.25 | 37.8 | 4391 | 105 | 1.63 | 9.14 | 1.02 | |
| 3c | <1.80 | | | | | <2.02 | <9.17 | | |
| 4a | 16.6 | 0.53 | 170.7 | 8047 | 83 | | 10.58 | 0.38 | |
| 7a | 15.70 | 0.80 | 54.5 | 4221 | 317 | | 10.02 | 0.25 | |
| 7c | 4.73 | 0.58 | 34.7 | 4401 | 124 | 1.51 | 9.59 | 0.10 | -0.23 |
| 10a | 2.72 | 0.49 | 9.3 | 5277 | 339 | <8.10 | 9.65 | -0.63 | -1.08 |
| 10c | 7.14 | 0.36 | 21.8 | 4612 | 359 | 4.81 | 9.70 | 0.14 | -0.12 |
| 11a† | 1.84 | 0.23 | 11.8 | 5433 | 171 | <2.70 | 9.41 | 0.23 | |
| 14b | 6.35 | 0.60 | 22.9 | 5867 | 383 | <2.50 | 9.60 | | |
| 14c | <1.50 | | | | | <3.60 | <8.76 | | |
| 16a | 42.86 | 1.29 | | 4056 | | | 9.98 | 0.55 | 0.43 |
| 16b | 3.44 | 0.67 | | 3871 | | | 9.21 | | |
| 16c | 62.95 | 1.53 | | 3835 | | | 10.15 | 0.54 | |
| 16d | 32.96 | 1.10 | | 3878 | | | 9.87 | 0.88 | |
| 19b† | 1.23 | 0.30 | 8.1 | 4255 | 146 | | 8.51 | 0.86 | |
| 21a | 14.86 | 1.20 | 53.0 | 7587 | 362 | | 10.31 | 0.05 | |
| 23b | 9.70 | 0.60 | 46.1 | 4914 | 318 | | 9.85 | 0.23 | |
| 23d | 2.15 | 0.20 | 24.8 | 4455 | 83 | | 8.92 | 0.37 | |
| 25a | 2.56 | 0.20 | 13.3 | 6272 | 193 | 1.68 | 9.39 | 0.55 | |
| 25c | 6.03 | 0.49 | 21.8 | 10894 | 394 | <1.62 | 10.07 | 0.37 | |
| 27b | 2.08 | 0.40 | 8.8 | 18516 | 311 | | 10.01 | 0.52 | |
| 31a | <2.64 | | | | | | <8.84 | | |
| 31c | 1.53 | 0.30 | 15.7 | 3987 | 148 | | 8.64 | | |
| 33c | 4.58 | 0.24 | 15.2 | 7787 | 362 | 19.1 | 9.63 | 0.23 | |
| 34b | 5.99 | 0.70 | 19.7 | 9393 | 364 | 3.68 | 9.86 | | |
| 37b | 8.65 | 0.40 | 19.6 | 6763 | 552 | 5.93 | 10.00 | -0.15 | |
| 38b | 7.87 | 1.40 | 33.5 | 8677 | 251 | | 10.08 | | |
| 40a | <1.32 | | | | | <2.88 | <8.90 | | |
| 40c | 9.7 | 0.65 | 34.9 | 6375 | 233 | | 9.94 | 0.14 | |
| 40d | 5.09 | 0.43 | 17.4 | 6729 | 295 | 3.09 | 9.57 | -0.01 | |
| 40e | 1.62 | 0.40 | 9.4 | 6480 | 66 | 1.23 | 8.98 | 0.65 | |
| 43a | 4.73 | 0.38 | 17.3 | 10026 | 256 | 1.49 | 9.86 | 0.33 | |
| 43b | 2.63 | 0.35 | 13.3 | 9920 | 278 | 1.82 | 9.66 | 0.45 | |
| 44a | 10.5 | 0.60 | 35.2 | 1239 | 269 | 3.65 | 9.13 | -0.18 | 0.06 |
| 44c | 7.63 | 0.50 | 50.2 | 1222 | 165 | <6.24 | 8.71 | 0.23 | 0.06 |

†not included in our final HCG sample

of only 14 galaxies with HI content known, due to the poor spatial resolution of the HI observations (Williams & Rood, 1987) and the lack of interferometric observations up to now. As already observed, we find a close correlation between the absolute $M_{H_2}$ content and the $L_{FIR}$. This correlation is usually interpreted as a relation between the fuel for star formation (molecular gas) and the tracer of that star formation (FIR luminosity) (Young et al., 1986). On Fig. 4 we present $L_{FIR}$ versus $M_{H_2}$ superposed with the linear fit (in log): $L_{FIR}$=40$M_{H_2}{}^{0.88\pm0.31}$. One of the galaxies (10a) exhibits a particular high $H_2$ content, without any counterpart of high $L_{FIR}$ luminosity, that could be due to a peculiar (not exponential-like) gas distribution, which would imply that our estimation of the total gas fails. Indeed that galaxy has a very large diameter relative to our beam. Mendes de Oliveira & Hickson (1994) remarked that it exhibits a peculiar HI profile.

### *3.5. Dust masses*

From the ratio of the IRAS $S_{60\mu m}$ and $S_{100\mu m}$ fluxes we have derived dust temperatures (cf Table 1), assuming $\kappa_\nu \propto \nu$. The average $T_d$ for the HCG galaxies with detected CO emission is $33 \pm 6$ K. By comparison, the average dust temperature for the starburst sample is $40 \pm 6$ K.

Knowing the dust temperature $T_d$ and the $S_{100\mu m}$ flux, we can derive the dust mass as

$$M_{dust} = 4.8 \times 10^{-11} \frac{S_\nu \, d^2_{Mpc}}{\kappa_\nu \, B_\nu(T_d)} \, M_\odot$$
$$= 5 \, S_{100} \, d^2_{Mpc} \, \{\exp(144/T_d) - 1\} \, M_\odot,$$

where $S_\nu$ is the FIR flux measured in Jy, $\kappa_\nu$ is the mass opacity of the dust, and $B_\nu(T_d)$ the Planck function. We used a mass opacity coefficient of 25 cm$^2$ g$^{-1}$ at 100$\mu$ (Hildebrand, 1983). In Table 1 we list the estimated dust masses, and in Fig. 5 we

**Table 3.** (continued)

| Name | $I_{CO}$ (K km s$^{-1}$) | $\delta I_{CO}$ (K km s$^{-1}$) | $T_p$ (mK) | $v_{CO}$ (km s$^{-1}$) | FWHM (km s$^{-1}$) | $I_{CO(2-1)}$ (K km s$^{-1}$) | Log($M(H_2)$) ($M_\odot$) | Log($L_{FIR}/M_{H_2}$) ($L_\odot/M_\odot$) | Log($L_{FIR}/(M_{gas})$) ($L_\odot/M_\odot$) |
|---|---|---|---|---|---|---|---|---|---|
| 44d | 1.79 | 0.19 | 18.5 | 1584 | 103 | 1.17 | 8.09 | 0.55 | -0.29 |
| 47a | 4.82 | 0.32 | 18.7 | 9630 | 321 | 1.23 | 9.92 | 0.35 | |
| 49a | <2.0 | | | | | <3.06 | <9.46 | | |
| 49b | <1.7 | | | | | <2.22 | <9.33 | | |
| 55a | <1.3 | | | | | | <9.68 | | |
| 57d | 1.45 | 0.24 | 10.0 | 9014 | 110 | 0.66 | 9.29 | | |
| 58a | 26.56 | 1.80 | 78.1 | 6132 | 510 | | 10.41 | 0.18 | 0.10 |
| 59a | 6.05 | 0.25 | 44.2 | 4130 | 125 | | 9.20 | 0.96 | 0.63 |
| 59d | <1.40 | | | | | <1.80 | <8.50 | | |
| 61c | 15.5 | 1.40 | 40.3 | 4034 | 484 | 7.50 | 9.82 | 0.59 | |
| 61d | <1.5 | | | | | <2.00 | <8.51 | | |
| 67b | 6.69 | 0.46 | 19.9 | 7599 | 298 | <2.94 | 10.07 | 0.21 | -0.16 |
| 67c | 0.85 | 0.20 | 11.9 | 7485 | 64 | <1.05 | 8.87 | | |
| 68c | 7.02 | 0.42 | 32.2 | 2302 | 214 | | 9.49 | 0.30 | -0.09 |
| 69a | 4.3 | 0.55 | 12.5 | 8848 | 386 | <5.22 | 9.92 | | |
| 69b | 3.27 | 0.17 | 14.7 | 8728 | 279 | 4.47 | 9.58 | 1.09 | |
| 71b | 4.88 | 0.65 | 24.3 | 9391 | 323 | | 9.79 | 0.82 | |
| 73a† | 2.85 | 0.45 | 28.7 | 5695 | 127 | | 9.44 | -0.12 | -0.87 |
| 75b | <2.40 | | | | | <4.86 | <9.66 | | |
| 75e | <1.60 | | | 12368 | | 0.53 | 9.14 | | |
| 78a† | 5.25 | 0.40 | 15.7 | 8628 | 363 | 5.00 | 9.97 | 0.39 | -0.10 |
| 79a | <1.70 | | | | | <2.52 | <8.68 | | |
| 79c | <2.10 | | | | | <3.90 | <8.77 | | |
| 80a | 10.40 | 0.60 | 29.7 | 9046 | 428 | 10.34 | 10.20 | 0.64 | |
| 82c | 5.14 | 0.60 | 23.0 | 10090 | 388 | 2.96 | 10.03 | 0.56 | |
| 88a | 5.96 | 0.80 | 16.2 | 5996 | 464 | 1.12 | 9.79 | 0.22 | |
| 89c | <2.22 | | | 8992 | | 0.56 | 8.96 | | |
| 92c | 4.95 | 0.70 | 17.2 | 6760 | 168 | | 9.97 | 0.18 | -0.09 |
| 93b | 9.95 | 0.52 | 46.5 | 4701 | 212 | 9.82 | 9.94 | 0.31 | 0.15 |
| 95b | <1.70 | | | | | <2.28 | <9.55 | | |
| 95c | 3.96 | 0.30 | 17.7 | 11579 | 302 | <2.46 | 10.02 | | |
| 95d | 1.07 | 0.20 | 8.9 | 12074 | 173 | <1.80 | 9.34 | | |
| 96a | 17.4 | 1.10 | 116.5 | 8666 | 192 | 13.74 | 10.57 | 0.54 | |
| 96c | 2.69 | 0.40 | 11.4 | 8808 | 320 | 3.34 | 9.47 | | |
| 100a | 5.38 | 0.80 | 21.7 | 5298 | 402 | | 9.55 | 0.72 | 0.31 |

†not included in our final HCG sample

**Table 4.** Average quantities[a] with their standard deviation.

| Sample | $M_{H_2}/L_B$ $M_\odot/L_\odot$ | $L_{FIR}/L_B$ | $L_{FIR}/M_{H_2}$ $L_\odot/M_\odot$ | $L_{FIR}/(M_{H_2}+M_{HI})$ $M_\odot/L_\odot$ | $(M_{H_2}+M_{HI})/L_B$ $M_\odot/L_\odot$ | $M_d/L_B$ K | $T_d$ |
|---|---|---|---|---|---|---|---|
| HCG | -0.61(0.39) | -0.16(0.45) | 0.39(0.33) | -0.02(0.40) | -0.42(0.22) | -3.42(0.36) | 33.1(5.7) |
| Control | -0.78(0.58) | -0.11(0.61) | 0.67(0.38) | 0.06(0.41) | -0.34(0.35) | -3.54(0.41) | 35.0(5.4) |
| Pairs | -0.57(0.45) | 0.33(0.48) | 0.91(0.43) | 1.04(0.37) | -0.47(0.31) | -3.37(0.40) | 34.9(6.0) |
| Starburst | -0.61(0.43) | 0.63(0.43) | 1.24(0.39) | 0.91(0.39) | -0.36(0.40) | -3.27(0.34) | 40.4(6.2) |
| Cluster | -1.08(0.36) | -0.31(0.40) | 0.77(0.37) | 0.42(0.35) | -0.73(0.34) | -3.78(0.30) | 33.2(4.7) |
| Dwarf | -1.65(0.88) | -0.34(0.59) | 1.38(0.68) | 0.13(0.43) | -0.32(0.65) | -4.11(0.67) | 38.1(7.2) |
| Elliptic | -1.65(0.77) | -0.46(0.62) | 1.19(0.48) | 0.39(0.32) | -0.64(0.24) | -4.07(0.63) | 33.1(5.2) |

a) All averages are logarithmic

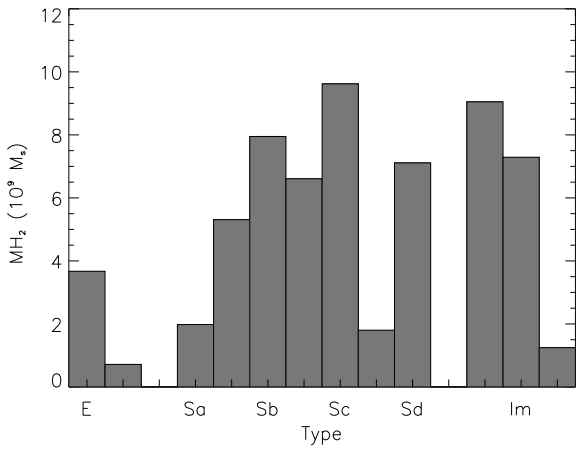


**Fig. 3.** Mean $H_2$ mass ($10^9$ $M_\odot$) versus galaxy morphological type for our HCG sample.

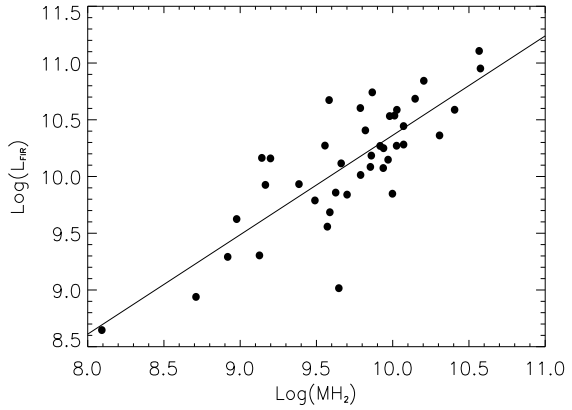


**Fig. 4.** The FIR luminosity versus the $H_2$ mass for our HCG sample. The least square linear fit is superposed.

plot the dust mass derived from the FIR flux versus the $H_2$ mass derived from the CO observations. The full line is a fit of the dust mass to the $H_2$ mass, corresponding to a simple proportionality between the two masses, with a molecular gas–to–dust mass ratio of 725 which is similar to the molecular gas–to–dust ratio of the control sample (741). The total gas–to–dust ratio is not reliable (high dispersion) given our small sample with FIR and HI available. We computed for all our samples the cumulative distribution of the ratio $M_{\rm H_2}/M_{\rm dust}$(log). It is clear from Fig. 8 that this ratio in all samples, except the dwarf and elliptic samples , follows the same distribution, the maximum $\chi^2$ with the HCG sample being 4.1 (probability 0.46) to be compared with the Table 5. Although there is some observational evidence in favor of a constant gas-to-dust ratio in galactic giant molecular clouds (GMCs), as shown by Sanders et al. (1991), a departure from this value could indicate that either a fraction of the FIR luminosity comes from dust associated with the diffuse atomic ISM or that the $H_2$/CO conversion factor is galaxy-dependent. Sanders et al. (1991) also suggest that the opacity coefficients could underestimate dust masses.

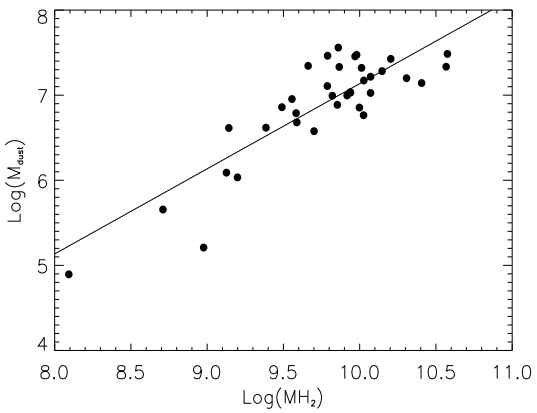


**Fig. 5.** The molecular mass derived from the CO intensities for our HCG sample, versus the dust mass derived from the FIR luminosity. The full drawn line represents a simple proportionality between the two mass estimates for a molecular gas–to–dust mass ratio of 725.

### *3.6. The CO(2-1)/CO(1-0) ratio*

We detected the $^{12}$CO(2→1) line in 26 galaxies only (55% detection rate). In the other CO detected galaxies, we have only an upper limit of the CO(2-1)/CO(1-0) ratio. In most cases, we observed only one position per galaxy: since the beam sizes are different for the two lines, we cannot determine the true line ratio, without a precise model of the source distribution. In any case, we measure an average raw line ratio of 0.74 $\pm$ 0.2, without beam correction. The true ratio will be obtained by dividing by a factor between 1 and 4, because of the factor 2 between the CO(2-1) and CO(1-0) linear beam size. It is thus certain that the CO emission is in general sub-thermally excited, as is frequently the case at large scale in galaxies (e.g. Braine & Combes 1992). There is only one exception, the galaxy 33c, where the true CO(2-1)/CO(1-0) ratio could be of the order of 1. It has been shown that the CO line ratio varies little with the interaction class of the galaxy (Casoli et al. 1988, Radford et al. 1991); it is not a good temperature indicator, but rather a density indicator (it is higher in the galaxy centers, as expected). As a matter of fact this global ratio cannot disentangle in any way the different excitation CO conditions in the galaxies (hot cores, diffuse component).

### *3.7. Correlation with the radio continuum flux*

We have plotted $M_{\rm H_2}$ versus the radio luminosity at 1.4 GHz of the detected compact group galaxies in Fig. 7. A clear correlation can be found, indicating that both are related to star-forming activity. Menon (1995) has shown that the total radio emission from the discs of HCG galaxies is significantly less than that of a comparable sample of isolated galaxies, while the reverse is true for the nuclear emission. He suggested that the nuclear radio emission is mainly due to star formation bursts and not due to nuclear activity. This is supported here from the good correlation between normalised molecular gas content and ra-

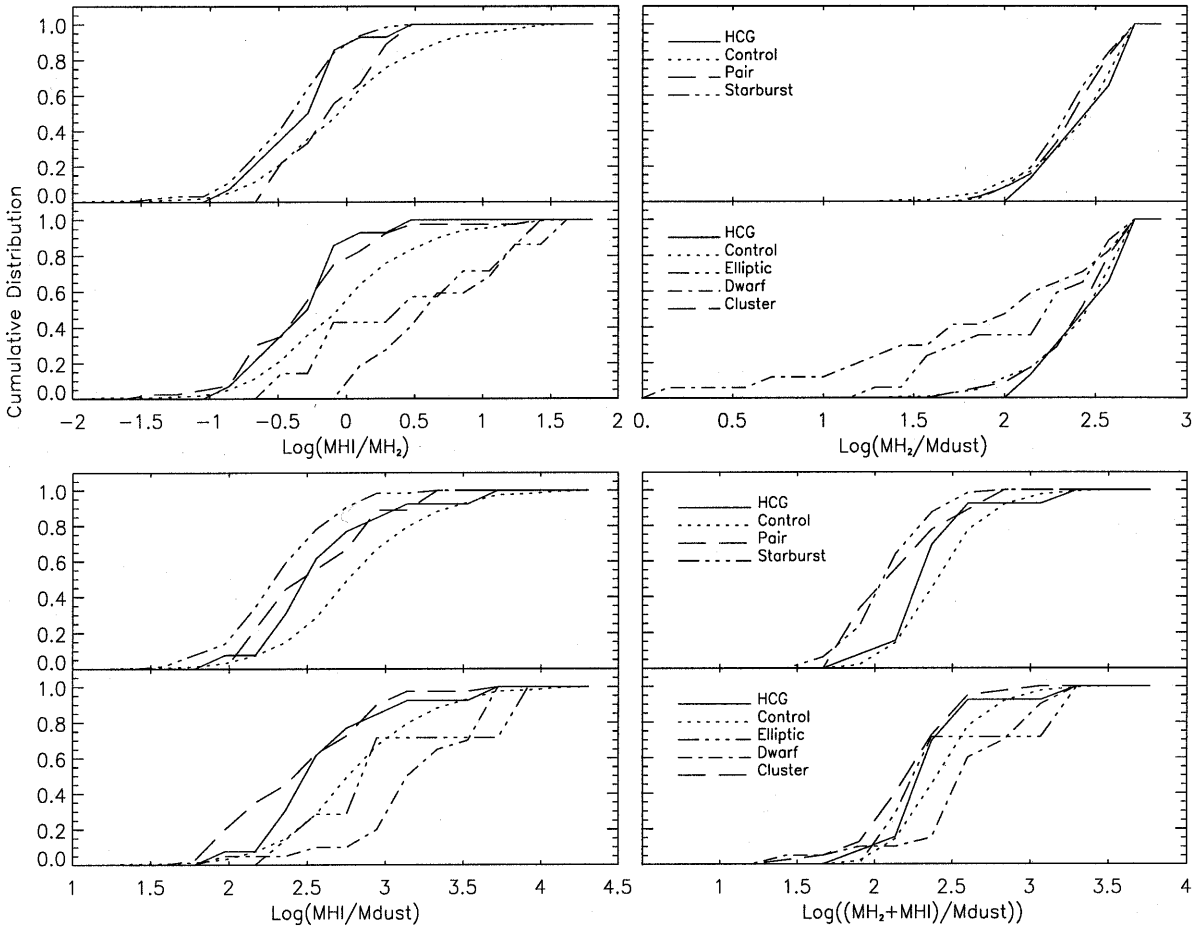


**Fig. 6.** The cumulative distributions for the different samples described in the text. Here are represented the ratio of the $H_2$, HI and dust masses.

dio power. AGN-powered radio emission should perturb this correlation, but this appears negligible here.

### *3.8. CO maps of a few objects*

Some of the Hickson groups are near enough to be resolved by our beam, and we mapped a few objects, in particular several galaxies in HCG16. This compact group appears as a unique condensation of active galaxies, containing one Seyfert 2 galaxy, two LINERS and three starbursts (Ribeiro et al 1996). The galaxy density is 217 gal Mpc$^{-3}$. Ponman et al (1996) detected a diffuse X-ray component corresponding to intra-cluster hot gas. We present in Fig. 9 the CO spectra towards the HCG16 galaxies. Some of them (16a and 16b) reveal several velocity components, which can be attributed to overlapping galaxies. 16c and 16d present a clear enhancement of their molecular content with an $M_{H_2}/L_B$ ratio equal respectively to -0.21 and -0.37 (log). These two galaxies exhibit optical starburst activity which indicates recent interaction, younger than $10^8$ yr (Ribeiro et al. 1996); while the galaxies 16a and 16b show tidal tails indicating a later interaction phase. They should already have suffered intense star formation and have consumed part of the fueling gas available. To our spatial resolution of 22″ we do not observe such a high central concentration of the molecular gas as for radio continuum emission (Menon, 1995).

### *3.9. About the compactness*

We plot in Fig. 8 the mean $M_{H_2}/L_B$ ratio versus the mean projected separation in the group. There is an enhancement of the $H_2$ content up to a mean separation of 30 kpc. This is an indication for the interaction intensity threshold to trigger inner gas flows by tidal interactions. Galaxies with a mean separation less than 25 kpc have $M_{H_2}/L_B$=-0.26 ($\pm$0.33), whereas galaxies with separation more than that distance have $M_{H_2}/L_B$=-0.66 ($\pm$0.37). It is interesting to note that the correlation is weaker when the closest projected separation is used instead of the mean separation in the group. This suggests that the enhancement is a function of the dynamics of the *whole* group in the case of the most compact groups, apart from possible strong binary interactions, as shown in HCG16. The $L_{FIR}/M_{H_2}$ ratio does not exhibit any dependence with the mean separation.

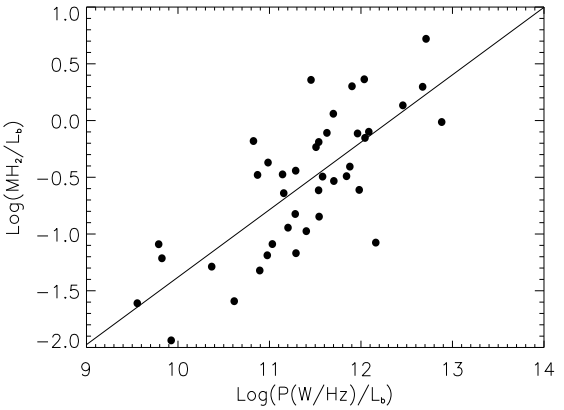


**Fig. 7.** The molecular mass, normalised to $L_B$, of HCG galaxies versus their radio continuum emission. The least square linear fit is overplotted.

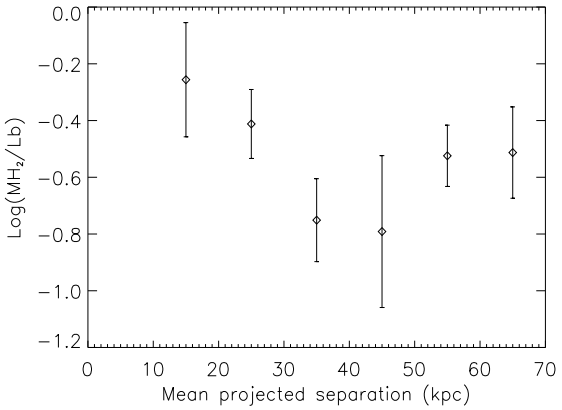


**Fig. 8.** $M_{H_2}/L_B$ ratio versus the mean separation in each group per bin of 10 kpc.

## 4. Discussion

### *4.1. Gas content*

To compare our HCG sample with the comparison samples we used the cumulative distributions for the different quantities. Performing Kolmogorov-Smirnov (KS) or $\chi^2$ test we check the hypothesis of a common underlying population for the different samples.

One of the result derived from the comparisons of Fig. 9 concerns the CO emission: there does seem to be an enhancement of $M_{H_2}$ in HCG galaxies with respect to a control sample which does not share the same underlying distribution (KS: 0.21 (0.05 significance), $\chi^2$: 15.66 (0.64 probability)). However HCG population seems to share the same distribution with starburst (KS: 0.12 (0.61), $\chi^2$: 9.65 (0.68)) and pair (KS: 0.22 (0.16), $\chi^2$: 11.30 (0.58)) samples. We present in Table 5 the KS and $\chi^2$ results for all coupled samples. The distribution functions of the HCG and control sample exhibit the main difference for the low $H_2$ content galaxies. Although the HCG sample does not exhibit a global FIR enhancement for all galaxies, as shown in Fig. 14, it appears that tidal interactions are efficient in Compact Groups, at least in the most compact ones as we have shown in the previous section. These tidal torques could drive the gas inwards, which might be related to the enhancement of radio continuum emission in the very center of these galaxies. The $H_2$ enhancement does not appear to be a bias from our FIR selected sample since it has a FIR distribution close to that of the control sample (KS: 0.14 (0.49)) but we will discuss afterwards about the Malmquist bias which could be an important limitation in this issue. We can point out that in case of a perturbed molecular gas distribution, our extrapolation for the total mass should fail. But in this case the conclusion would remain similar, leading that time to an enhancement of the molecular content in the *center*. This enhancement of molecular gas is also supported by the enhancement of dust mass. Its cumulative distribution in HCG also follows that of the starburst (KS: 0.18 (0.38),$\chi^2$: 8.65 (0.69)) and pair (KS: 0.11 (0.91),$\chi^2$: 9.08 (0.72)) samples. In spite of the poor HI data, we can point out that the similarity between these three populations (HCG, pairs and starbursts) for the total gas ($M_{H_2}$+$M_{HI}$)/$L_B$ ratio is even tighter (KS: 0.12 (0.99), $\chi^2$: 5.51 (0.79), gathering pair and starburst samples in one sample). The case of dwarfs, exhibiting a very peculiar molecular gas-to-dust ratio, can be interpreted in terms of the low metallicity of these objects and will be discussed in a forthcoming paper (Leon et al., 1997).

Thus in a galaxy group two mechanisms are at play concerning the gas evolution: on one hand tidal interactions enhance the molecular content by driving gas inwards and on the other hand the Intra Cluster Medium strips off the outer gas, reducing the eventual molecular content. It appears that the former dominates for the most compact groups, while for the least compact groups the picture is mitigated. Nevertheless it can be emphasized that the enhancement of dust mass gives us a hint about evidence of tidal interactions in the HCG sample.

### *4.2. Completeness of the distribution*

We check the completeness of the $M_{H_2}/L_B$ distribution function (top left of Fig. 9) by simulating the distribution function taking into account the threshold of detection for that quantity. The minimum temperature detection is 4 mK in our observations. Then we consider the distance distribution for the galaxies to be uniform up to 150 Mpc or gaussian with the parameters of our sample. The linewidth distribution has been fitted to the blue luminosity $L_B$ with a power law (Tully-Fisher-like relation with $L_B \propto \Delta V^{4.3}$). Then inclination angle is distributed uniformly between 0 and 90 degrees. The blue luminosity is distributed with a gaussian distribution ($< \log(L_B) >= 10.22$, $\sigma_{L_B} = 0.16$). For each $\log(M_{H_2}/L_B)$ bin, the fraction of realisations above the threshold detection is computed to estimate the completeness of our sample. Results are displayed in Fig. 12 for $10^4$ realisations. Gaussian and uniform distance distributions are two extremes chosen to estimate the weight of the distance parameter: the 50 % level of completeness is $\log(M_{H_2}/L_B) = -1.8$ for the uniform case and -1.5 for the gaussian case.

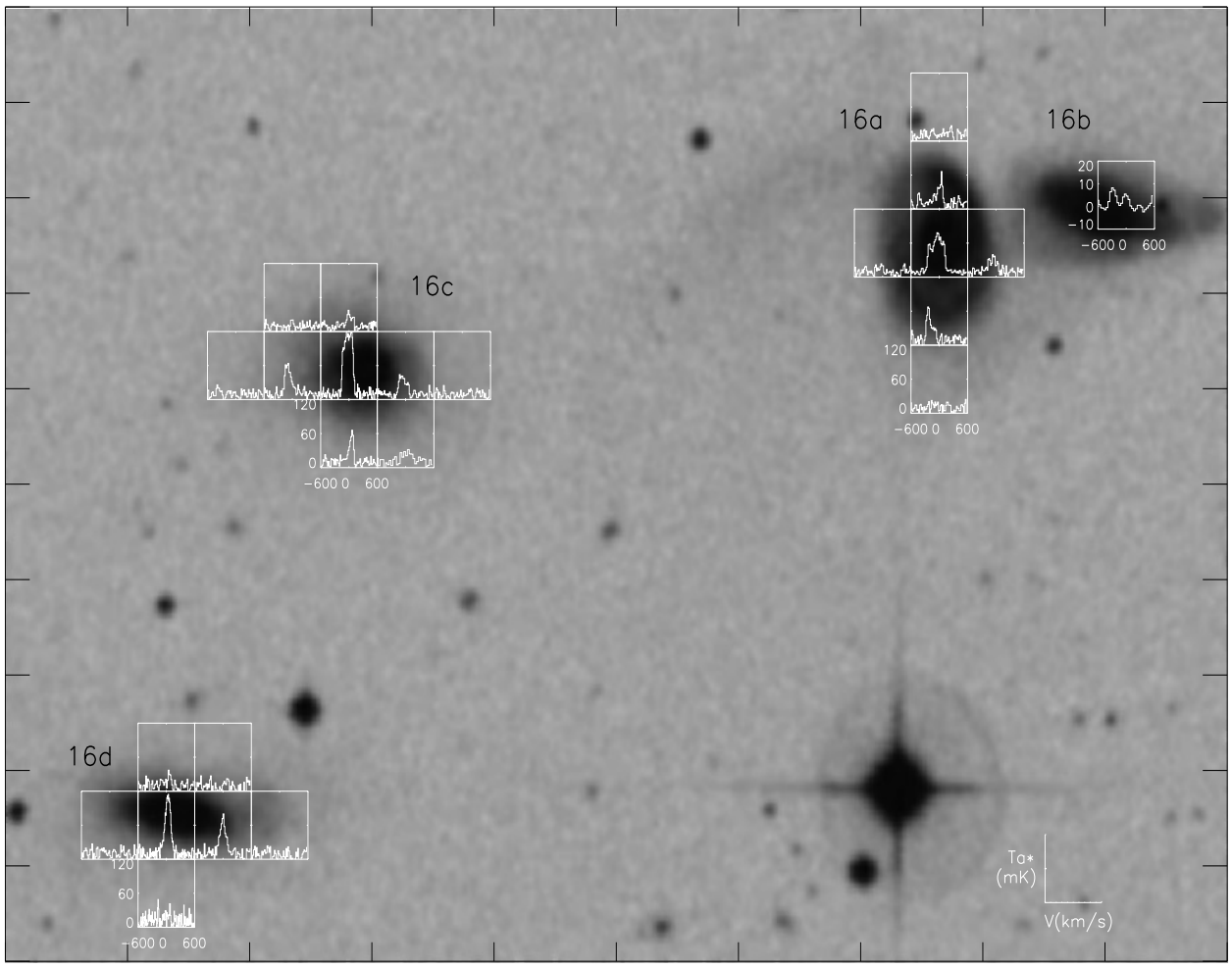


**Fig. 9.** Spectra towards the HCG16 galaxies, superposed on an optical image of the group (taken from the DSS). The velocity is in km s$^{-1}$centered on the recession velocity of each galaxy and the y-axis is in units of $T_{\rm A}^{*}$ (mK).

**Table 5.** KS and $\chi^2$ statistics for the $\log(M_{\rm H_2}/L_{\rm B})$ distribution between every two different samples. In the upper part we give the $\chi^2$ value and the probability (brackets) of the test, in the lower part is the maximum difference between two cumulative distributions and the KS significance (brackets).

| | HCG | control | starburst | pair | cluster | dwarf | elliptic |
|---|---|---|---|---|---|---|---|
| HCG | | 15.66(0.64) | 9.65(0.68) | 11.30(0.58) | 34.36(0.02) | 47.75(0.01) | 40.61(0.02) |
| control | 0.21(0.05) | | 19.08(0.52) | 22.65(0.33) | 32.00(0.10) | 57.55(0.00) | 63.06(0.00) |
| starburst | 0.12(0.71) | 0.16(0.14) | | 9.98(0.66) | 32.49(0.04) | 52.06(0.00) | 49.10(0.00) |
| pair | 0.22(0.16) | 0.18(0.15) | 0.10(0.95) | | 25.11(0.08) | 39.22(0.03) | 34.73(0.04) |
| cluster | 0.59(0.00) | 0.40(0.00) | 0.51(0.00) | 0.50(0.00) | | 24.88(0.19) | 18.96(0.26) |
| dwarf | 0.66(0.00) | 0.50(0.00) | 0.65(0.00) | 0.67(0.00) | 0.41(0.01) | | 16.90(0.49) |
| elliptic | 0.68(0.00) | 0.53(0.00) | 0.66(0.00) | 0.61(0.00) | 0.33(0.11) | 0.18(0.89) | |

Assuming that our control sample is complete, we compute a cumulative distribution biased by the completeness function of Fig. 12. Fig. 13 shows the result where it appears that the Malmquist bias in our sample, spread over a large distance range, can explain part of the apparent enhancement of molecular gas in the HGGs. However the control sample, assumed to be complete, is not likely to be so for the low values of $\log(M_{\rm H_2}/L_{\rm B})$) where the samples are the most different. Similarly the $\log(M_{\rm dust}/L_{\rm B})$ distribution is affected by the Malmquist bias (Verter, 1993), but the point is that the cumulative distribution is lower than the control distribution on the whole range of variation up to higher values, leading to a suggestion of a real enhancement of the dust material in the HCGs. The close correlation between dust and molecular gas suggests that the $H_2$ content is really enhanced in the HCGs. *As it has been shown previously, that enhancement is only significant for the most*

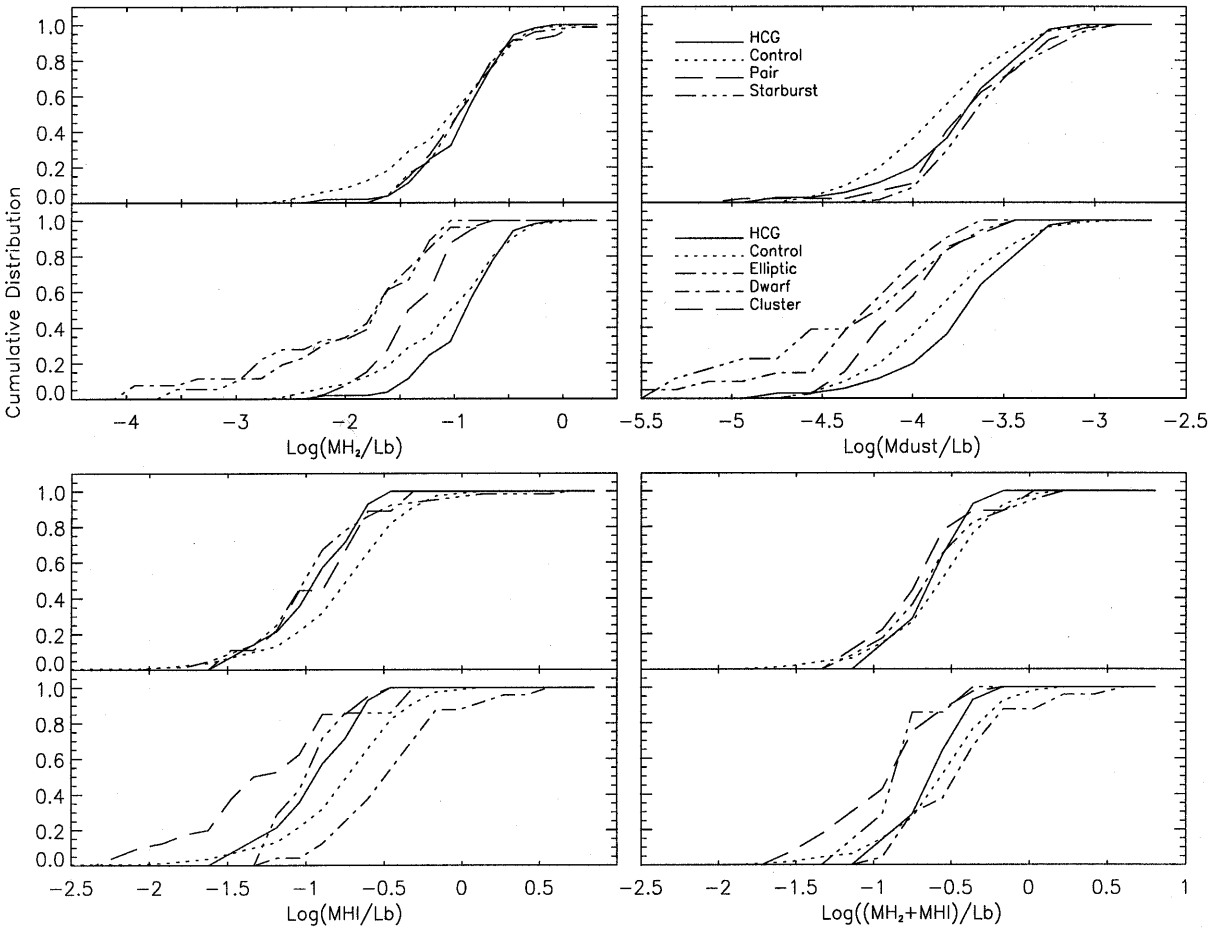


**Fig. 10.** Cumulative distribution of the different samples for the $H_2$, HI and dust masses. The top graphs compare the HCG with control, pair and starburst ensembles; the bottom ones to the other categories.

*compact groups in their merging phase, confusing somewhat the question of molecular gas enhancement in the whole HCG sample.*

### *4.3. High SFE due to artificially low gas content*

What can also be seen in Fig. 11(a) is the large dispersion of the SFE as defined by the $L_{\rm FIR}/M_{\rm H_2}$ ratio: a large number of galaxies are deficient in CO emission, leading to a depressed $M_{\rm H_2}/L_{\rm B}$ ratio and large SFE. This large dispersion is mainly due to the dwarf and elliptical samples, but also to small galaxies in the control sample; we have checked that the objects with high SFE at moderate $L_{\rm FIR}/L_{\rm B}$ have a lower $L_{\rm B}$ than average. This phenomenon disappears when the total gas content is considered instead of the mere $H_2$ content, as shown in Fig. 11(b) and (d). It is striking that the total normalised gas content is almost a constant, independent of $L_{\rm FIR}/L_{\rm B}$. There is one exception for the cluster population where the stripping of the neutral and molecular content is at play. We find a deficiency of the molecular content in these galaxies, which seems related to a lower $L_{\rm FIR}$ luminosity (Horellou et al. 1995). All that suggests the importance of HI in star formation as a source of fueling, through the conversion $H_2 \leftrightarrow$ HI, and the higher reliability of the star formation indicator $L_{\rm FIR}/(M_{\rm H_2}+M_{\rm HI})$. A least square fit yields the relation $L_{\rm FIR}/(M_{\rm H_2}+M_{\rm HI}) \simeq 2.4(\frac{L_{\rm FIR}}{L_{\rm B}})^{0.69\pm0.10}$ for all the samples gathered.

The good correlation between the normalised $M_{\rm H_2}$ and $L_{\rm FIR}$ could be in a large part due to the dependence of both quantities on the metallicity and temperature of the interstellar medium. It is now well established that the CO to $H_2$ conversion ratio is strongly dependent on metallicity (e.g. Rubio et al 1993), as well as the dust-to-gas ratio (and therefore the FIR luminosity). As shown on Fig. 8, all the cumulative distributions for the molecular gas-to-dust ratio are highly correlated, ($\chi^2$: all, except dwarf and elliptic samples, $< 6$. (probability $> 0.54$)). While the dependence of $L_{\rm FIR}$ on temperature is direct, that of the CO emission is more complex. Low brightness temperatures of the CO lines are obtained either for cold gas, or diffuse gas; the rotational levels of the molecule are excited by collision, and diffuse molecular clouds are generally sub-thermal. The use of a standard CO to $H_2$ conversion ratio is then problematic. For thermalised dense gas however, the CO emission is directly proportional to the gas temperature. The metal abundance and the gas recycling are closely related to the IMF and evolution of

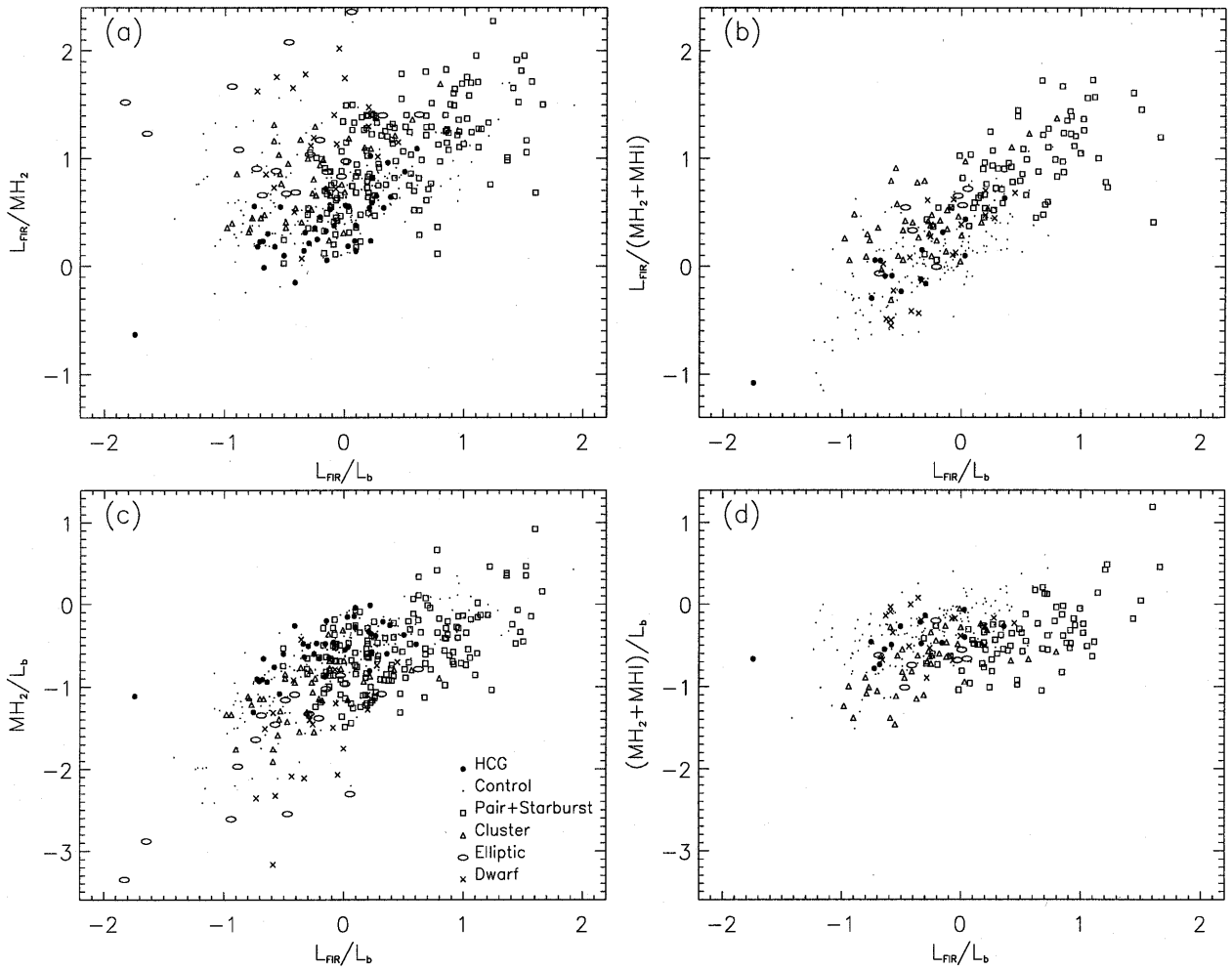


**Fig. 11a–d.** Comparison between our HCG sample and other CO-detected samples: **a** Star Formation Efficiency (SFE) as represented by $L_{\rm FIR}/M_{\rm H_2}$ versus $L_{\rm FIR}/L_{\rm B}$. **b** same as **a** but including the HI gas in the definition of the SFE **c** $M_{\rm H_2}$ versus $L_{\rm FIR}$ normalised to blue luminosity. **d** total gas content ($M_{\rm H_2}$ +M(HI)) versus $L_{\rm FIR}$ normalised to blue luminosity.

the MF. High mass stars (M$>$ 5M$_\odot$) are active on short time scales ($< 10^8$ yrs) whereas low mass stars have an influence on much longer time scales (Vigroux et al. 1996). Thus the CO abundance is very dependent on the star formation rate, and the CO/$H_2$ conversion ratio could be very variable, particularly for galaxies with recent star formation episodes (e.g. Casoli et al 1992, Henkel & Mauersberger 1993).

### *4.4. Far-infrared and star-forming activity*

Given the enhancement in CO emission detected in HCG with respect to a control sample and the strong correlation between the radio continuum, CO and the FIR for HCG spirals it would appear that the lack of enhancement of the total FIR emission in HCG galaxies is due to lack of spatial resolution of IRAS measurements. This is particularly important if the FIR is mainly enhanced in the central regions of the galaxies. ISO observations might allow to check this assertion.

The consequence of an enhanced $M_{\rm H_2}$ without FIR enhancement is a lower star forming efficiency for HCG, as displayed in Fig. 14. This property might appear surprising, but disappears when the total gas content is taken into account (this result should be taken with caution, since only 14 galaxies have a well-defined HI content in our HCG sample).

We have tested the correlations of the star formation indicators, with and without account of the atomic phase, with the dust temperature, in Fig. 15. Both quantities correlate well with $T_{\rm d}$: for all samples together we find a relationship flatter than Young et al. (1989), i.e. $L_{\rm FIR}/M_{\rm H_2} \propto {T_{\rm d}}^{3.8\pm0.7}$, but with differences and large dispersions among categories: for the HCG sample alone $L_{\rm FIR}/M_{\rm H_2} \propto {T_{\rm d}}^{2.5\pm2.5}$ and for the starburst sample $L_{\rm FIR}/M_{\rm H_2} \propto {T_{\rm d}}^{3.2\pm1.8}$. Sage (1993) pointed out that a single dust temperature is an "average" of the cold dust and warm dust associated respectively with the quiescent molecular clouds and the clouds with massive star forming ones. Devereux & Young (1990) emphasized that high mass ($> 6$ M$_\odot$) O and B stars are responsible for high $L_{\rm FIR}$ ($> 10^9$ L$_\odot$) and $H_\alpha$ luminosities, ad-

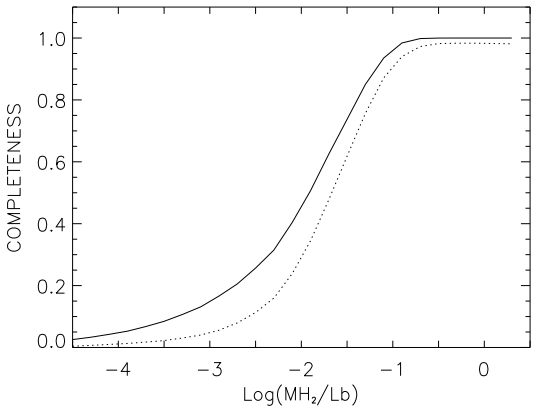


**Fig. 12.** Completeness distribution of the $\log(M_{\rm H_2}/\ L_{\rm B})$ quantity for our sample. Uniform (solid line) and gaussian (dashed line) distribution for the simulated distance in our realisations are shown.

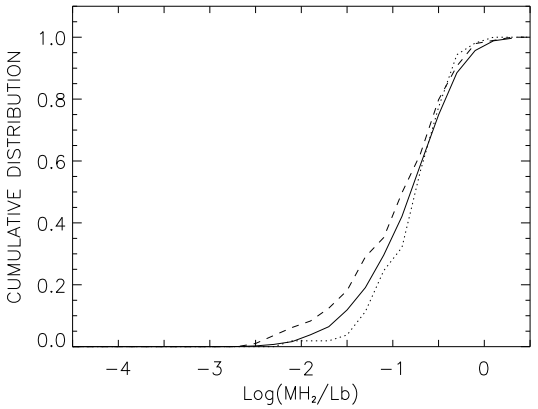


**Fig. 13.** Cumulative distribution (solid line) of the $\log(M_{\rm H_2}/\ L_{\rm B})$ quantity simulated from the completeness of the distribution (see text) and the observed distribution for the HCG (dot line) and the control samples (dashed line).

vocating a two-component model: one dust component heated by high mass stars ($T_{\rm d}\sim$ 50-60 K) and the other heated by the interstellar radiation field ($T_{\rm d}\sim$ 16-20 K). The low mean temperature of the HCG sample ($T_{\rm d}\approx$ 33 K) suggests that the $L_{\rm FIR}$ luminosity is coming from an important quiescent molecular phase, together with the "cirrus" phase associated with diffuse atomic hydrogen. It could explain why the *global* $L_{\rm FIR}$ luminosity does not fit with a high star formation population, without excluding star formation towards the center, as revealed by radio continuum. In a recent study, Lisenfeld et al. (1996) find the same $L_{\rm FIR}/L_{2.4GHz}$ ratio for starburst interacting and normal galaxies. From this, we could infer that the enhanced radio continuum emission from the center of HCG galaxies should be accompanied with an enhanced central FIR luminosity. The constancy of the $L_{\rm FIR}/L_{2.4GHz}$ ratio has been interpreted as being due to a strong and fast ($10^7$ yrs) increase of the magnetic field at the beginning of the starburst, together with a time-scale of variation of the star-formation rate longer than some $10^7$ yrs.

### *4.5. Fate of the HCG*

The enhancement of the $H_2$ content in the most compact groups suggests that tidal interactions in HCG are efficient in driving the gas inwards. This is also a confirmation that at least some groups are actually compact and not only projections along the line of sight. These very compact groups should merge through dynamical friction on a short time scale (a few $10^8$ yrs, cf Barnes 1989). A conclusion from the present work is that the most compact of these groups have concentrated an important amount of molecular gas without initiating yet important star formation. However they must correspond to a short duration phase just before merging and enhanced star-formation. It is tempting to identify the next phase of this process to the Ultra Luminous Infra Red Galaxies (ULIRGs). The latter have their infrared luminosity powered by massive star formation (Lutz et al. 1996) with an important consumption of molecular gas. Sanders et al (1988) have shown that many ULIRGs are interacting/merging galaxies; recently Clements & Baker (1996) extended that to the vast majority of the ULIRGs sample. Some of these systems, with luminous masses ranging up to few $10^{11}{\rm M}_\odot$, should represent the remnant of some compact group which has undertaken multiple mergers on a very short time-scale ($\sim 10^8$ yrs). The FIR luminosity of the final ULIRGs should be a function of the spiral fraction in the parent group, the most powerful ULIRGs being the result of the merging of typically four gas-rich spirals. As pointed out earlier the spatial distribution of interstellar matter within galaxies will play an important role in the rate of fuelling of starbursts during interactions.

But does the expected rate of ULIRGs formation via CG merging match the presently observed frequency of these objects? The answer is very uncertain, since the actual fraction of very compact groups, on the point of merging, is not known. This fraction cannot be close to 1, since there would be too large a discrepancy between the expected and observed number of ultra luminous galaxies and their remnants (e.g. Williams & Rood 1987, Sulentic & Rabaça 1994). Simulations of galaxy formation and large-scale structures evolution have suggested that some of the CGs could be filaments of galaxies seen end-on (Hernquist et al. 1995). This idea has been studied further by Pildis et al. (1996): if it is true that galaxies that will form a compact group spend a large fraction of their time first in a filament, this filament will appear as a CG in projection only for less than 20% of cases. Then the galaxies will fall into a real CG, and this phase corresponds to at least 30% of their lifetime. Although these figures are model dependent, they suggest that the majority of HCG in the sky are physically compact groups. The time-scale of merging can then depend highly on initial conditions, and in particular on the elliptical fraction, which may alleviate the over-merging problem (e.g. Governato et al. 1991, Garcia-Gomez et al. 1996).

The threshold in mean galaxy separation for the enhancement of $H_2$ suggests that it corresponds to the last stage of the life of the compact group, when each galaxy is undertaking frequent and strong tidal effects. In Fig. 16 we plot the histogram of the mean projected separation of the whole sample of HCGs from

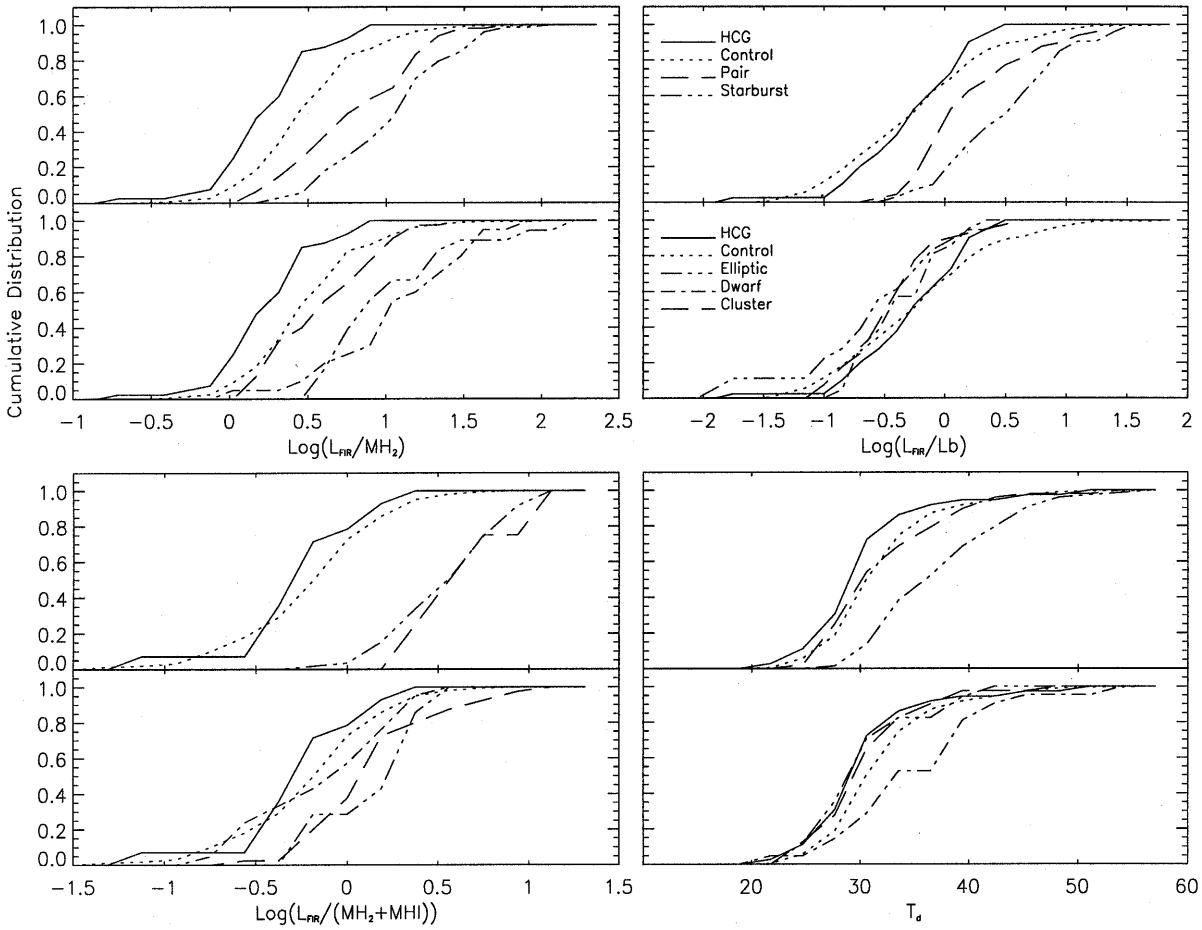


**Fig. 14.** Cumulative distribution of the different samples for the FIR-related values.

Hickson et al. (1992): there is a significant cut-off at short separation at approximatively 20-30 kpc, which must correspond to a short life time for very compact configurations. We suggest that this cut-off corresponds to the acceleration of the merging process, and at the same time to significant inward gas flows, that account for our observations. Dynamically, such an exponential acceleration of the collapse is predicted by simulations and analytic models of satellite decay through dynamical friction (see for example Leeuwin & Combes 1997). This rapid acceleration has been interpreted through the excitation of numerous high-order resonances for a satellite at about twice the primary radius (e.g. Tremaine & Weinberg 1984).

## 5. Conclusion

From our survey of CO emission in 70 galaxies belonging to 45 Hickson compact groups, we have detected 57 objects. We find in average that the gas and dust contents $M_{\rm H_2}/L_{\rm B}$ and $M_{\rm dust}/L_{\rm B}$ show evidence of enhancement with respect to our control sample. This result however is somewhat weakened due to the Malmquist bias in our sample. For the most compact groups the enhancement is more clear. On the contrary, the global far-infrared flux does not appear to be enhanced with respect to the control sample. The FIR and $T_{\rm d}$ distribution indicates that the FIR luminosity is coming essentially from a cold dust component heated by the interstellar radiation field. From the general correlation between FIR and radio contiuum power we suggest that only the very centers of some groups are experiencing star formation and are sites of enhanced FIR emission. IRAS spatial resolution is not sufficient to show this directly. Statistical tests show that the HCG gas and dust contents are closer to that of pair and starburst galaxies, revealing the efficiency of tidal interactions in driving the gas inwards in compact group galaxies. We find a stronger $H_2$ enhancement for the CGs having a short mean separation ($< 30$ kpc). We suggest that these most compact, high-$H_2$ content groups, may be in a final merging phase, just before the starburst phase, that will lead them in a very short time-scale to the ULIRGs category.

The comparison of the various samples suggest that the *total* gas content ($H_2$+HI) should be taken into account to estimate the star formation efficiency. The corresponding SFE indicator, $L_{\rm FIR}/(M_{\rm H_2}+M_{\rm HI})$, should be more reliable, and allow us to avoid some systematic effects depending on metallicity and temperature.

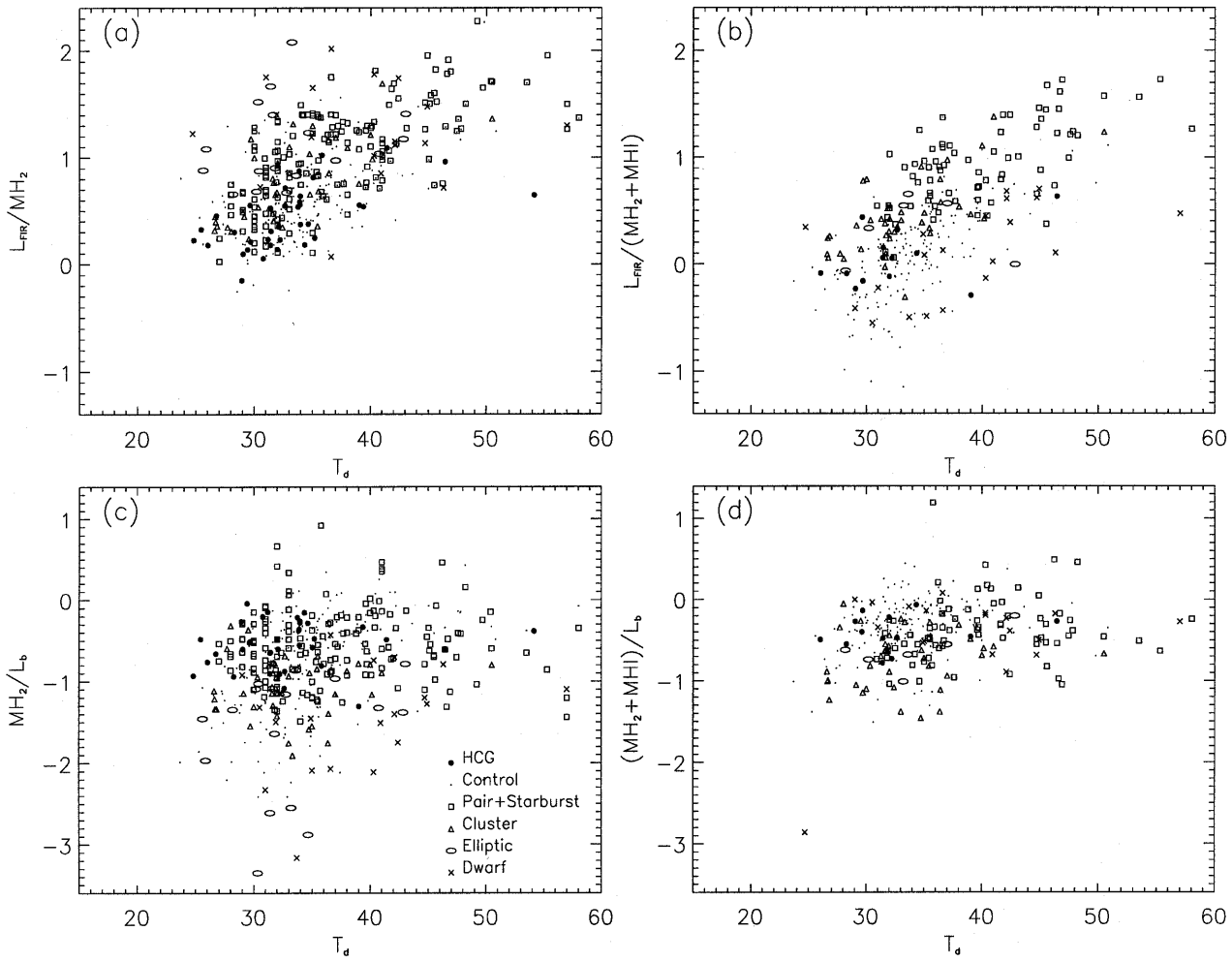


**Fig. 15a–d.** Comparison between the HCG sample and other CO-detected samples: **a** $L_{\rm FIR}/M_{\rm H_2}$ versus $T_{\rm d}$. **b** $L_{\rm FIR}/(M_{\rm H_2}$ + M(HI)) versus $T_{\rm d}$. **c** $M_{\rm H_2}/L_{\rm B}$versus $T_{\rm d}$. **d** $(M_{\rm H_2}+M_{\rm HI})/L_{\rm B}$versus $T_{\rm d}$.

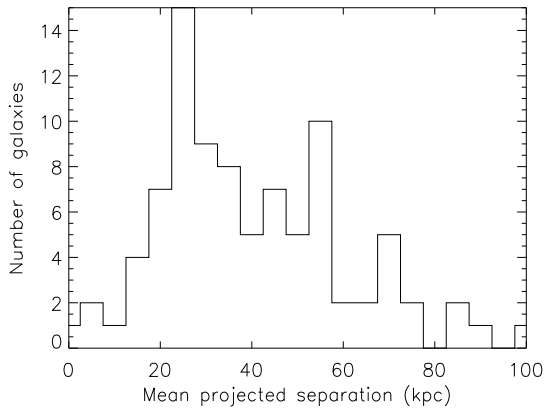


**Fig. 16.** Histogram of the mean projected separation for the whole HCG sample, limited to 100 kpc, from Hickson et al. (1992).

*Acknowledgements.* We are very grateful to the staff at Pico Veleta for their help during these observations and especially to R. Moreno and R. Frapolli. We also thank the anonymous referee whose suggestions greatly improved this paper. This work largely benefitted from the LEDA, NED and SIMBAD data bases. This investigation was also supported by a grant from the Natural Sciences and Engineering Research Council of Canada to T.K.M.

## Appendix A: $H_2$ mass determination

We follow Gordon et al. (1992) to derive $H_2$ masses from $^{12}$CO(1→0) line observations. Our temperature unit is expressed in $T_{\rm A}^*$ antenna temperature scale which is corrected for atmospheric attenuation and rear sidelobes. The radiation temperature $T_R$ of the extragalactic source is then:

$$T_R = \frac{4}{\pi}(\frac{\lambda}{D})^2 \frac{K}{\eta_A}\frac{T_A}{\Omega_S} \qquad \text{(A1)}$$

where $\lambda$ is the observed wavelength (2.6 mm), D is the IRAM radio telescope diameter (30 m), K is the correction factor for the coupling of the source with the beam, $\eta_A$ is the apperture efficiency (0.55) at 115 GHz, $T_A$ is an antenna temperature which is $F_{eff}T_A^*$ in the IRAM convention, explicitely

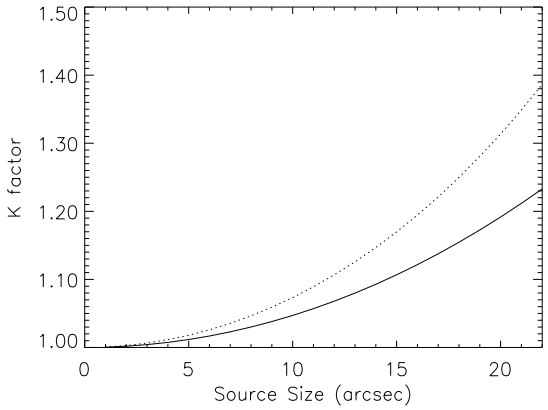


**Fig. 17.** Correction factor K in the case of an exponential (solid line) and an uniform (dot line) source distribution

$T_A$=0.92$T_A^*$, and $\Omega_S$ is the source size. Without taking into account cosmological correction, because of low redshift, column density of molecular hydrogen it written down as

$$N(H_2) = 2.3 \times 10^{20} \int_{line} T_R dv \ (\mathrm{mol.cm^{-2}}) \quad \text{(A2)}$$

where $dv$ is the velocity interval . In Eq. A1 K$\equiv \Omega_s/\Omega_\Sigma$ is the factor which corrects the measured antenna temperature for the weighting of the source distribution by the large antenna beam in case of a smaller source. We have defined the source solid angle

$$\Omega_S \equiv \int_{source} \phi(\theta,\psi) d\Omega \quad \text{(A3)}$$

where $\phi(\theta,\psi)$ is the normalized source brightness distribution function. The beam-weighted source solid angle is

$$\Omega_\Sigma \equiv \int_{source} \phi(\theta,\psi) f(\theta,\psi) d\Omega \quad \text{(A4)}$$

where $f(\theta,\psi)$ denotes the normalized antenna power pattern (Baars, 1973). Experiments have shown that we can approximate $f$ by a gaussian beam. As mentionned in Sect. 3.3 an exponential law of scale length h=$D_B$/10 is taken to model the source distribution function. As long as the source size is smaller than the beam size we have

$$K = \frac{\int_0^{\theta_s/2} sin(\theta) e^{-\frac{10\theta}{\theta_s}} d\theta}{\int_0^{\theta_s/2} sin(\theta) e^{-\frac{10\theta}{\theta_s} - \ln(2)(\frac{2\theta}{\theta_b})^2} d\theta} \quad \text{(A5)}$$

where $\theta_b$ and $\theta_s$ are the beam and the source sizes. We present in Fig. 17 the plot of K in the case of exponential and uniform source distributions, for the IRAM-30m beam at 115 GHz (22 $''$). In the case of a source larger than the beam size it is more difficult to compute the coupling of the beam to the source region since contributions from error beam can be quite significant to the resulting spectra. A simple representation of the overall beam, including the error beam, is not available to correct that coupling. Since in our sample, galaxies are at most a few beam sizes large we used Eq. A5 integrated on the beam size to derive the K factor for galaxies with larger optical diameters.

If $I_{CO}$ is the velocity-integrated temperature in $T_A^*$ scale and given the IRAM-30m parameters, the total mass of $H_2$ is then given by

$$M(H_2) = 5.86 \times 10^4 D^2 K I_{CO} \ (\mathrm{M_\odot}) \quad \text{(A6)}$$

with the distance D in Mpc.

## References


Allam S., Assendorp R., Longo G. et al: 1996 A&AS 117, 39
Baars J.W.M.: 1973, IEEE Trans. Ant. Prop. AP-21, 461
Barnes J.: 1989, Nature 338, 123
Barnes J., Hernquist L.: 1982, ARA&A 30, 705
Boselli A., Mendes des Oliveira C., Balkowski C., Cayatte V., Casoli F.: 1996, A&A 314, 738
Braine J., Combes F.: 1992, A&A 264, 433
Braine J., Combes F.: 1993, A&A 269, 7
Casoli F., Boissé P., Combes F., Dupraz C.: 1991, A&A 249, 359
Casoli F., Dupraz C., Combes F.: 1992, A&A 264, 55
Cayatte V., van Gorkom J.H., Balkowski C., Kotanyi C.: 1990, AJ 100, 604
Clements D.L., Baker A.C.: 1996, A&A 314, 5
Combes F., Dupraz C., Casoli F., Pagani L.: 1988, A&A 203, L9
Combes, F., Prugniel P., Rampazzo R., Sulentic J.W.: 1994, A&A 281,725
Dressler A.: 1984, ARAA 22, 185
Garcia-Gomez C., Athanassoula E., Garijo A.: 1996, A&A 313, 363
Gordon M.A., Baars J.W.M., Cocke W.J.: 1992, A&A 264, 337
Gourgoulhon E., Chamaraux P., Fouqué P.: 1992, A&A 255, 69
Governato F., Chincarini G., Bhatia R.: 1991, ApJ 371, L15
Greve A., Panis J-F., Thum C.: 1996 A&AS 115, 379
Henkel C., Mauersberger R.: 1993, A&A 274, 730
Hernquist L., Katz N., Weinberg D.H.: 1995, ApJ 442, 57
Hickson P.: 1982, ApJ 255, 382
Hickson P., Kindl E., Auman J.R: 1989, ApJS 70, 687
Hickson P., Mendes de Oliveira C., Huchra J.P., Palumbo G.G.C.: 1992, ApJ 399, 353
Hickson P.: 1990, in IAU Coll 124, "Paired and Interacting Galaxies", ed. J.W. Sulentic & W.C. Keel, p. 77
Hildebrand, R.H. 1983, QJRAS 24, 267
Israel F.P., Tacconi L.J., Baas, F.: 1995, A&A 295, 599
Kenney J.D.P., Young J.S.: 1988, ApJS 66, 261
Leeuwin F., Combes F.: 1997, MNRAS 284, 45
Leon S., Combes F., Junqueira S., 1997, in preparation
Lisenfeld U., Voelk H-J., Xu C.: 1996, A&A 314, 745
Lutz, D., Genzel R., Sternberg A. et al: 1996, A&A 315, L137
Mamon G.: 1986, ApJ 307, 426
Mamon G.: 1987, ApJ 321, 622
Mamon G.: 1992 in "Physics of nearby galaxies: nature or nurture?", ed. T.X. Thuan, C. Balkowski & J. Tran Thanh Van, Editions Frontières, Gif-sur-Yvette, p. 367
Mamon G.A.: 1994, in "N-body Problems and Gravitational Dynamics", ed. F. Combes & E. Athanassoula, p. 188
Mauersberger R., Guélin M., Martin-Pintado J. et al: 1989 A&AS 79, 217
Mendes de Oliveira C., Hickson P.: 1991, ApJ 380, 30
Mendes de Oliveira C., Hickson P.: 1994, ApJ 427, 684

Mendes de Oliveira C.: 1992, PhD Thesis, British Columbia Univ.
Menon T.K.: 1995, MNRAS 274, 845
Menon T.K., Hickson P.: 1985, ApJ 296, 60
Menon T.K.: 1991, ApJ 372, 419
Mulchaey J.S., Davis D.S., Mushotzky R.F., Burstein D. 1993, ApJ 413, L81
Pildis R.A., Bregman J.N., Schombert J.M.: 1995, AJ 110, 149
Pildis R.A., Evrard A.E., Bregman J.N.: 1996, AJ 112, 378
Ponman T.J., Bertram D.: 1993, Nature 363, 51
Ponman T.J., Bourner P.D.J., Ebeling H., Böhringer H.: 1996, MNRAS 283, 690
Ribeiro A.L.B., Carvalho R.R., Coziol R., Capelato H.V., Zepf S.: 1996, ApJ 463, L5
Rood H.J., Williams B.A.: 1989, ApJ 339, 772
Rubio M., Lequeux J., Boulanger F.: 1993, A&A 271, 9
Rubin V.C., Hunter D.A., Ford W.K.: 1991, ApJS 76, 153
Sage L.J., Salzer J.J., Loose H.-H.: Henkel C 1992, A&A 265, 19
Sage L.J.: 1993, A&A 272, 123
Sanders D.B., Soifer B.T., Elias J.H et al: 1988, ApJ 325, 74
Sanders D.B., Scoville N.Z., Soifer B.T.: 1991, ApJ 370, 158
Solomon P.M., Sage L.J.: 1988, ApJ 613, 334
Strong A.W., Bloemen J.B.G.M., Dame T.M. et al: 1988 A&A 207, 1
Sulentic J.W., de Mello Rabaça, D.: 1993, ApJ 410, 520
Sulentic J.W., Rabaça, C.: 1994, ApJ 429, 531
Thronson, H.A., Telesco, C.M. 1986, ApJ 311, 98
Tinney C.G., Scoville N.Z., Sanders D.B., Soifer B.T.: 1990, ApJ 362, 473
Verdes-Montenegro L. et al: 1997, A&A sub
Verter, F., 1993, ApJ, 402, 141
Vigroux L., Mirabel F., Altieri B. et al: 1996, A&A 315, L93
Wiklind T., Combes F., Henkel C.: 1995, A&A 297, 643
Williams B.A., Rood H.J.: 1987, ApJS 63, 265
Xu C., Sulentic J.W.: 1991, ApJ 374, 407
Young J.S., Xie S., Kenney J.D.P., Rice W.L.: 1989, ApJS 70, 699
Young J.S., Xie S., Tacconi L. et al: 1995, ApJS 98, 219
Young J.S., Allen L, Kenney J.D.P., Lesser A., Rownd B.: 1996, AJ 112, 1903
Young, J.S., Knezek, P. 1989, ApJ 347, L55
Yun M.S., Verdes-Montenegro L., Del Olmo A., Perea J.: 1997, ApJ 457, L21